FEBS Letters

REVIEW ARTICLE

RNA-virus proteases counteracting host innate immunity

Jian Lei[1] and Rolf Hilgenfeld[1,2]

1 Institute of Biochemistry, Center for Structural and Cell Biology in Medicine, University of Lübeck, Germany
2 German Center for Infection Research (DZIF), Hamburg - Lübeck - Borstel - Riems Site, University of Lübeck, Germany

Correspondence
R. Hilgenfeld, Institute of Biochemistry, Center for Structural and Cell Biology in Medicine, University of Lübeck, Ratzeburger Allee 160, 23562 Lübeck, Germany
Fax: +49 451 3101 3104;
Tel: +49 451 3101 3100
E-mail: hilgenfeld@biochem.uni-luebeck.de

(Received 26 July 2017, revised 21 August 2017, accepted 22 August 2017, available online 15 September 2017)

doi:10.1002/1873-3468.12827

Edited by Wilhelm Just

Virus invasion triggers host immune responses, in particular, innate immune responses. Pathogen-associated molecular patterns of viruses (such as dsRNA, ssRNA, or viral proteins) released during virus replication are detected by the corresponding pattern-recognition receptors of the host, and innate immune responses are induced. Through production of type-I and type-III interferons as well as various other cytokines, the host innate immune system forms the frontline to protect host cells and inhibit virus infection. Not surprisingly, viruses have evolved diverse strategies to counter this antiviral system. In this review, we discuss the multiple strategies used by proteases of positive-sense single-stranded RNA viruses of the families Picornaviridae, Coronaviridae, and Flaviviridae, when counteracting host innate immune responses.

Keywords: cleavage of host proteins; innate immunity; viral protease

Proteases of positive-sense single-stranded RNA ((+)ssRNA) viruses

Since about two decades, emerging and re-emerging viruses have caused an increasing number of disease outbreaks in humans. In particular, emerging RNA viruses pose great threats to public health, for example, Ebola virus, Zika virus (ZIKV), and Middle-East respiratory syndrome coronavirus (MERS-CoV). The latter two are positive-sense single-stranded RNA ((+)ssRNA) viruses. We will briefly introduce the proteases of three (+)ssRNA virus families here, namely Picornaviridae, Coronaviridae, and Flaviviridae. This will be followed by a description of the complex signaling pathways that lead from recognition of the viral intruders to the production of antiviral cytokines, such as type-I and type-III interferons (IFNs). Finally, we will discuss the mechanisms by which the viral proteases interfere with these signaling pathways.

The Picornaviridae family includes a large number of small nonenveloped (+)ssRNA viruses with a genome size between 7.5 and 10 kb. As of March 2017, this family contains 35 genera with 80 species [1]. The genera *Enterovirus*, *Hepatovirus*, *Aphthovirus*, and *Cardiovirus* have been well investigated. Picornaviruses can cause several severe diseases in man and animals, such as poliomyelitis, hepatitis, and encephalitis. The viral genome usually encodes a polyprotein comprising regions P1, P2, and P3 (Fig. 1A) [2,3]. The P1 region includes the structural proteins, while the latter two comprise nonstructural proteins, including the enzymes required for polyprotein processing and RNA replication. P1, P2, and P3 are further cleaved by viral proteases into mature proteins. P1 is digested to 1A (also known as VP4), 1B (VP2), 1C (VP3), and 1D (VP1); P2 is processed to 2A, 2B, and 2C; whereas P3 becomes 3A, 3B, 3C, and 3D [2,3]. Picornaviruses encode up to three proteases, the 2A protease ($2A^{pro}$), the 3C protease ($3C^{pro}$), and – in case of some family members (e.g. the genera *Aphthovirus* and *Cardiovirus*) – the leader protease (L^{pro}) (Fig. 1A) [4].

Abbreviations
ADNP, activity-dependent neuroprotective protein; BVDV, bovine viral diarrhea virus; CSFV, classical swine fever virus; DENV, dengue virus; DUB, deubiquitination; HCV, hepatitis C virus; IFN, interferon; ISG, IFN-stimulated gene; MERS-CoV, Middle-East respiratory syndrome coronavirus; M^{pro}, main protease; pDCs, plasmacytoid dendritic cells; PL^{pro}, papain-like protease; SARS-CoV, severe acute respiratory syndrome coronavirus; TBEV, tick-borne encephalitis virus; WNV, West Nile virus; YFV, yellow fever virus.

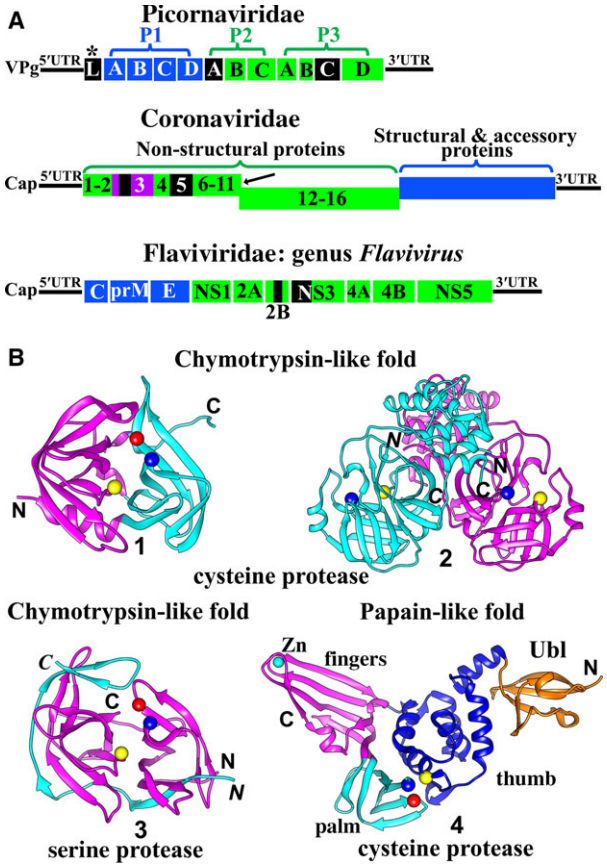

Fig. 1. (A) Genome organization of picornaviruses, coronaviruses, and flaviviruses. All structural and accessory proteins are shown in blue. Nonstructural proteins are shown in green, with the exception of proteases, which are shown in black. Picornaviridae : The 5′ end of the picornavirus genomic RNA is covalently bound to VPg (viral protein genome-linked). The genome encodes a polyprotein comprising the three regions P1 (structural proteins), P2, and P3 (nonstructural proteins). Generally, two viral proteases, $2A^{pro}$ and $3C^{pro}$, cleave the polyprotein into mature proteins. P1 is processed to yield 1A (VP4), 1B (VP2), 1C (VP3), and 1D (VP1); P2 is processed to 2A, 2B, and 2C; while P3 cleavage products are 3A, 3B, 3C, and 3D. *In some picornavirus genera (e. g. *Aphthovirus, Cardiovirus*), a third viral protease exists, the leader protease (L^{pro}). It auto-cleaves itself from the polyprotein. Coronaviridae:CoVs possess the largest genome of all known RNA viruses. The 5′ genomic RNA carries a methylated cap. Two open-reading frames (ORFs), 1a and 1b, occupy the 5′-terminal two thirds of the CoV genome. ORF1a encodes the polyprotein 1a (Nsp1-11), while ORF1a plus ORF1b are translated into the polyprotein 1ab (Nsp1-16); this involves a (-1) ribosomal frameshift overreading the stop codon of ORF1a (indicated by the black arrow). The 3′-proximal third encodes the structural and accessory proteins. The polyproteins pp1a and pp1ab are processed by the viral proteases PL^{pro} (within Nsp3; Nsp3 is purple) and M^{pro} ($3CL^{pro}$, Nsp5). The genomes of members of the Flaviviridae differ between genera. Here, a genome of a member of the genus *Flavivirus* is shown as an example. The 5′-capped genome encodes a polyprotein, which is cleaved into three structural proteins as well as seven nonstructural proteins by host and viral proteases. Flaviviruses have only one protease, the $NS2B/NS3^{pro}$. NS2B is a cofactor for the NS3 serine protease. (B) Structures of proteases of +ssRNA viruses. The fold of most RNA-virus proteases belongs to either the chymotrypsin-like class or the papain-like class. The chymotrypsin fold consists of two β-barrel domains, while the typical papain-like fold contains an α-helical domain and a predominantly β-sheet domain. The catalytic residues are located in the cleft between the two domains in both chymotrypsin-like and papain-like proteases. Picornavirus $2A^{pro}$, $3C^{pro}$, coronavirus $3CL^{pro}$ (M^{pro}), HCV and pestivirus NS3/NS4A^{pro}s, as well as flavivirus $NS2B/NS3^{pro}$, adopt the chymotrypsin-like fold, whereas picornavirus L^{pro} and coronavirus PL^{pro} feature the papain-like fold. 1) The structure of enterovirus D68 $3C^{pro}$ [19] (PDB entry: 3ZV8). The Cα atoms of the catalytic triad Cys–His–Glu are shown as yellow, blue, and red spheres, respectively. 2) The structure of transmissible gastroenteritis virus (TGEV, a CoV) $3CL^{pro}$ (M^{pro}) [24] (PDB entry: 1LVO). Dimerization of the $3CL^{pro}$ (M^{pro}) is a prerequisite for its activity. The two protomers are displayed in cyan and purple. The catalytic dyad Cys–His (Cα atoms shown as yellow and blue spheres) is located within the chymotrypsin-like subdomain of each monomer. An additional α-helical domain also exists in each protomer. 3) The structure of Zika virus $NS2B/NS3^{pro}$ [22] (PDB entry 5LC0). The NS3 protease is shown in purple and the NS2B cofactor is in cyan. The Cα atoms of the catalytic triad Ser–His–Asp are shown as yellow, blue, and red spheres, resp. 4, The structure of MERS-CoV PL^{pro} [26] (PDB entry 4P16). In the coronavirus PL^{pro}, the β-sheet domain is larger than in the canonical papain-like fold and divided into two subdomains, fingers (purple) and palm (cyan); together with the thumb subdomain (α-helical domain; blue), an extended right-hand fold is the result. A ubiquitin-like (Ubl) domain (orange) is located in the N-terminal region of the PL^{pro}. The Cα atoms of the catalytic triad residues Cys–His–Asp are shown as yellow, blue, and red spheres, resp. All figures in (B) have been prepared by using UCSF Chimera [183].

The Coronaviridae family is divided into two subfamilies, Coronavirinae and Torovirinae [1]. Two recently emerged human coronaviruses from the subfamily Coronavirinae, severe acute respiratory syndrome coronavirus (SARS-CoV) and MERS-CoV, can cause severe pneumonia. In particular, the latter virus frequently also leads to renal failure [5]. Coronaviruses are enveloped +ssRNA viruses and have the largest genome (26–32 kb) of all known RNA viruses. The 5′-terminal two thirds of the genome contain the two open-reading frames (ORFs) 1a and 1b. ORF1a codes for polyprotein 1a containing nonstructural protein 1–11 (Nsp1–11), while ORF1a and ORF1b together encode polyprotein 1ab comprising Nsp1–16. This latter mechanism features a (-1) ribosomal frameshift overreading the stop codon of ORF1a (Fig. 1A) [6]. The 3′-proximal third encodes the structural and accessory proteins [7,8]. These two polyproteins are processed into 15 or 16 mature Nsps to form the replication/transcription complex. This step is performed by two types of viral proteases, namely, one or two papain-like proteases (PL^{pro}(s)) located within Nsp3, and a main protease (M^{pro}) (Nsp5), which is frequently also called '3C-like protease' ($3CL^{pro}$) (Fig. 1A; see [9] for a review).

The family Flaviviridae includes four genera: *Hepacivirus*, *Flavivirus*, *Pestivirus*, and *Pegivirus*. Here, we discuss viral proteases from the former three genera. Since the genome organization and the proteases are different in these three genera of the Flaviviridae family, we will introduce them separately.

Viruses from the genus *Hepacivirus* are enveloped (+) ssRNA viruses. The best characterized member of this genus is hepatitis C virus (HCV). This virus can lead to acute and chronic hepatitis. About 71 million people have chronic hepatitis C infection worldwide (www.who.int, last accessed on August 16, 2017). The genome of HCV is about 9.6 kb in size and encodes a polyprotein precursor that is processed by host and two viral proteases to yield four structural (C, E1, E2, and p7) and six nonstructural proteins (NS2, NS3, NS4A, NS4B, NS5A, and NS5B). These two viral proteases are the NS2 autoprotease ($NS2^{pro}$) and the NS3/NS4A protease ($NS3/NS4A^{pro}$) [10,11]. NS4A is a cofactor for the NS3 protease. In HCV, the latter enzyme is also called $NS3/4A^{pro}$ in many publications; however, we will use '$NS3/NS4A^{pro}$' in what follows, in order to be consistent with the $NS2B/NS3^{pro}$ notation in the flaviviruses.

Viruses of the genus *Flavivirus* are also enveloped (+) ssRNA viruses. Members of the genus include dengue virus (DENV), West Nile virus (WNV), yellow fever virus (YFV), tick-borne encephalitis virus (TBEV), Zika virus (ZIKV), etc. Flaviviruses are mainly transmitted by arthropods, such as mosquitoes or ticks. Many of the mosquito-borne family members are highly endemic in the tropics and subtropics, whereas TBEV is prevalent in Central and Eastern Europe. The ~11-kb genome of flaviviruses encodes a polyprotein that is cleaved into three structural (C, prM, and E) and seven nonstructural proteins (NS1, NS2A, NS2B, NS3, NS4A, NS4B, and NS5) by host and viral proteases (Fig. 1A). The genus *Flavivirus* only has one protease, $NS2B/NS3^{pro}$ [12].

Viruses of the genus *Pestivirus* mainly infect mammals, such as cattle and swine. Bovine viral diarrhea virus (BVDV) and classical swine fever virus (CSFV) belong to this genus. The genome of pestiviruses encodes a polyprotein that is processed by viral and host proteases into 12 mature proteins (N^{pro}, C, E^{rns}, E1, E2, p7, NS2, NS3, NS4A, NS4B, NS5A, and NS5B). In this genus, three proteolytic enzymes, the N-terminal protease (N^{pro}), the $NS2^{pro}$, and the $NS3/NS4A^{pro}$, have been identified [13–15].

Although the primary structures of proteases in these three (+)ssRNA virus families are very different from one another, the three-dimensional structures of most proteases belong to either the chymotrypsin-like fold or the papain-like fold (Fig. 1B). The typical chymotrypsin fold consists of two β-barrel domains, each containing six β-strands. The catalytic residues are located in the cleft between these two domains. Picornavirus $2A^{pro}$ [16], $3C^{pro}$ [17–19], HCV $NS3/NS4A^{pro}$ [20], flavivirus $NS2B/NS3^{pro}$ [21,22], and pestivirus $NS3/NS4A^{pro}$ [23] adopt this fold; however, the former two enzymes are cysteine proteases, while the latter three are serine proteases. The coronavirus M^{pro} ($3CL^{pro}$) also possesses a chymotrypsin-like fold, but with an additional α-helical domain; furthermore, dimerization of this cysteine protease is a prerequisite for its activity (Fig. 2B) [9,24]. However, the picornavirus L^{pro} [4,25] and the coronavirus PL^{pro} [9,26,27] feature a papain-like fold. The canonical papain-like fold contains an α-helical and a predominantly β-sheet domain, with the active site located in the cleft between them. This is exactly what is found in the picornavirus L^{pro} [4,25], whereas in the coronavirus PL^{pro}, the β-sheet domain is larger and further divided into two subdomains: fingers and palm. Together with the thumb subdomain (α-helical domain), they form an extended right-hand fold. In addition, a ubiquitin-like (Ubl) domain is located at the N terminus of the PL^{pro} (Fig. 1B) [9,26,27].

The various pathways to interferon expression in the host innate immune system

Viral infection will trigger immune responses. The host immune system consists of innate and adaptive

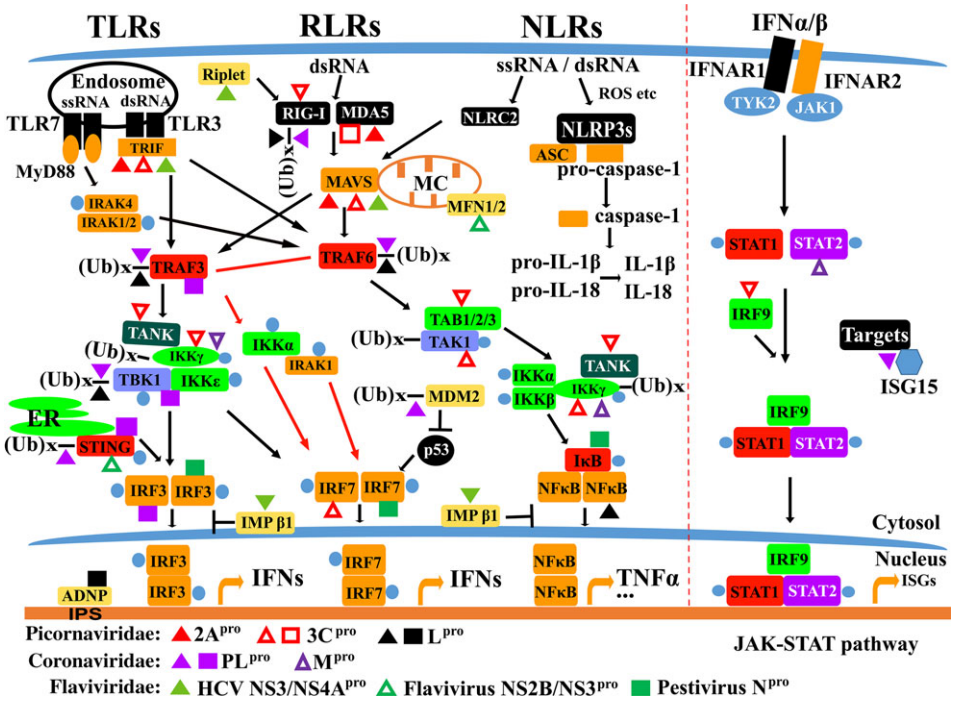

Fig. 2. Schematic overview of host innate immune pathways and their disruption by proteases of RNA viruses. The actions of viral proteases of three (+)ssRNA virus families, namely Picornaviridae, Coronaviridae, and Flaviviridae, are illustrated by triangle and square symbols. Triangles indicate cleavage of the target protein, while squares symbolize interaction with this protein in the absence of cleavage. Blue spheres indicate phosphorylation, and $(Ub)_x$ means polyubiquitination. (A) The TLR (Toll-like receptor), RLR (retinoic acid-inducible gene-I (RIG-I)-like receptor), and NLR (nucleotide-binding oligomerization domain (NOD)-like receptor) signaling pathways. TLR7 detects ssRNA and triggers downstream signaling *via* the adaptor, MyD88 (myeloid differentiation primary response gene 88). Subsequently, MyD88 recruits IRAK4 (interleukin-1 receptor-associated kinase 4) to activate IRAK1/2, then IRAKs dissociate from MyD88 and bind to TNF receptor-associated factor 6 (TRAF6). TRAF6 activates TAK1 (TGF-β-activated kinase 1). TAK1 further recruits TAB1/2/3 (TAK1-binding protein 1/2/3), to activate IKKα/β/γ (IκB kinase alpha, beta, and gamma; IKKγ is also named NEMO). Then, the IKKs mediate the phosphorylation of IκB, the NF-κB inhibitor. Phosphorylated IκB is degraded and releases NF-κB to induce production of TNFs (tumor necrosis factors) and other cytokines. This pathway thus comprises TLR7→MyD88→IRAK4/1/2→**TRAF6**→TAK1/TAB1–3→IKKα/β/γ→IκB→NF-κB. Also, TRAF6, IRAK4, TRAF3, IKKα, and IRAK1 form a complex. In this complex, both IKKα and IRAK1 activate the IRF7 (interferon regulatory factor 7) but not the IRF3 pathway (see red arrows). TLR3 detects dsRNA and triggers TRAF3 and TRAF6 by the mediator, TRIF (TIR domain-containing adaptor protein-inducing IFNβ). TRAF3 activates the TBK1/IKKε (TANK-binding kinase 1/IκB kinase epsilon)-mediated IRF3/7 pathway. TANK (TRAF family member-associated NF-κB activator) and IKKγ can activate TBK1/IKKε. TBK1/IKKε further stimulate the IRF3/7 pathway. In addition, STING (stimulator of interferon genes) can upregulate IRF3 signaling. The main cascade of this pathway thus comprises TLR3→TRIF→**TRAF3**→TBK1/IKKε→IRF3/7. TRAF6 and TRAF3 are typed in bold to indicate that they are located at central positions of pathways. The downstream cascade of TRAF6 activating the NF-κB pathway is the same as for the TLR7 pathway. RLRs detect ssRNA/dsRNA and trigger the activation of TRAF3 and TRAF6 by the mediator, MAVS (mitochondrial antiviral-signaling protein; also known as IPS-1, Cardif, VISA). The downstream signaling pathway is the same as for the TLR3 pathway. NLRs include NLRP3 and NLRC2 (also named NOD2). NLRP3 does not directly bind the viral RNA. The viral ssRNA or dsRNA causes many intracellular changes (such as reactive oxygen species (ROS) formation and lysosomal maturation), NLRP3 is sensitive to these changes and forms oligomers interacting with ASC (apoptosis-associated speck-like protein) and procaspase-1, collectively called 'inflammasome complex'. Subsequently, procaspase-1 is activated, thus leading to the maturation of pro-IL-1β and pro-IL-18. NLRC2 directly interacts with ssRNA, then it recruits MAVS to activate the IRF3 pathway. Also, it can activate TRAF6 to stimulate the NF-κB pathway. (B) The JAK-STAT signaling pathway. IFNα or IFNβ are produced *via* the IRF3/7 pathway. They bind the IFNAR1/2 (interferon alpha/beta receptor 1/2), leading to the activation of TYK2 (tyrosine kinase 2) and JAK1 (Janus kinase 1). These kinases phosphorylate STAT1 (signal transducer and activator of transcription 1) and STAT2. Subsequently, the phosphorylated STAT1/2 interact with IRF9 to form ISGF3 (IFN-stimulated gene factor 3). This ternary complex enters the nucleus and promotes the expression of ISGs (interferon-stimulated genes), such as ISG15, to establish the antiviral status. ISG15 covalently binds target proteins (ISGylation). Coronavirus PL^{pro} can remove ISG15 from ISGylated proteins. Other proteins and abbreviations in this figure: Riplet: an E3 ubiquitin ligase and upstream regulator of RIG-I; MFN 1/2: mitofusins 1/2. MFN1 and MFN2 regulate mitochondrial fusion; MFN1 is required for the RLR signaling pathway; IMPβ1: importin β1, a nucleocytoplasmic transport receptor, plays roles in the nucleocytoplasmic trafficking of IRF3 as well as NF-κB p65; MDM2: a p53 degradation stimulator blocks the p53–IRF7–IFNβ signaling pathway; ADNP: activity-dependent neuroprotective protein, a transcription factor, can bind to IFNα promoter sites (IPS) upon induction by L^{pro}; MC: mitochondrion; ER: endoplasmic-reticulum.

immunity. The innate immune system is the first-line defense to counteract viral invasion. When viruses enter host cells or replicate in them, various pathogen-associated molecular patterns (PAMPs) of viruses will be detected by the corresponding pattern-recognition receptors (PRRs) of the host. Subsequently, PRRs stimulate the different innate immune signaling pathways to produce various antiviral cytokines, including type-I and type-III IFNs. Type-I IFNs include multiple IFNα subtypes and IFNβ, which are produced by virtually all cell types. However, plasmacytoid dendritic cells (pDCs) are the dominant producers of type-I IFNs [28]. Type-III IFNs comprise IFNλ1-4 and can also be produced by pDC cells [29]. Following their production, IFNs stimulate the antiviral response by binding to different receptors located on the surface of host cells. IFNα/β bind to interferon alpha/beta receptors 1 and 2 (IFNAR1 and 2) (Fig. 2) [30], while IFNλ interacts with interferon lambda receptor 1 and the interleukin 10 receptor subunit beta (IFNLR1 and IL10Rβ) [29]. Although the receptors are different between type-I and type-III IFNs, they both activate the JAK-STAT (Janus kinase 1-signal transducer and activator of transcription 1) pathway to establish the antiviral state [29]. Thus, when activated as a consequence of the interaction of IFNα/β with IFNAR1/2, JAK1 and TYK2 (tyrosine kinase 2) phosphorylate STAT1 and STAT2. Subsequently, STAT1/2 interact with IRF9 (interferon regulatory factor 9) to form ISGF3 (IFN-stimulated gene factor 3). This ternary complex enters the nucleus and activates the expression of various ISGs (IFN-stimulated genes), such as ISG15. Finally, ISGs utilize autocrine and paracrine signaling to establish an antiviral state in surrounding cells.

Three main PRRs are involved in recognizing RNA viruses, namely Toll-like receptors (TLRs), retinoic acid-inducible gene-I (RIG-I)-like receptors (RLRs), and nucleotide-binding oligomerization domain (NOD)-like receptors (NLRs) [31–33]. Each of them can trigger the immune response by specific signaling pathways (Fig. 2). The former two PRRs are connected to the expression of type-I and type-III IFNs, ISGs, and tumor necrosis factors (TNFs), while NLRs mainly affect interleukin-1β (IL-1β) and IL-18 maturation [33–36].

Toll-like receptors (TLRs)

TLRs are transmembrane glycoprotein receptors. Different TLRs can be localized to the surface of the cell or to intracellular endosomes as well as lysosomes; therefore, they can detect various pathogens outside and inside of host cells [37,38]. TLRs comprise three subdomains: the N-terminal PAMP-binding region (PBR), which includes multiple leucine-rich repeats (LRRs), the middle transmembrane domain, and the C-terminal Toll/IL-1R homology (TIR) domain (Fig. 3) [38]. The N-terminal domain is used to bind PAMPs, while the C-terminal domain is involved in initiating the signaling cascades. In man, a total of 10 TLRs have been characterized [39]. TLR3, 7, 8 detect various RNA viruses and TLR9 detects DNA viruses [37]; in particular, TLR3 is mainly responsible for recognizing dsRNA while TLR7 detects ssRNA [33,37]. However, TLR3 and TLR7 utilize different downstream adaptors to activate the IRF3/7 or the NF-κB signaling pathway.

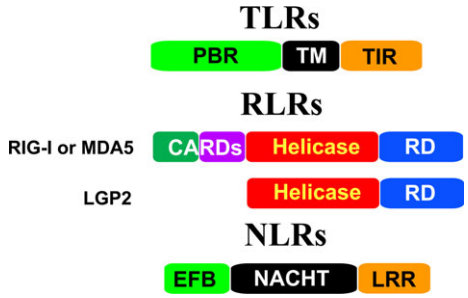

Fig. 3. Schematic presentation of individual TLR, RLR, and NLR domains. TLRs contain three domains: the N-terminal PAMP-binding region (PBR), the transmembrane region (TM), and the C-terminal intracellular Toll/IL-R homology (TIR) domain. RIG-I and MDA5 comprise an N-terminal two-CARDs (caspase-recruiting domains) domain, the central helicase domain, and the C-terminal repressor domain (RD). The CARDs domain is absent in LGP2. NLRs have various domain architectures. They mainly contain three domains: the variable N-terminal effector-binding domain (EFB), the middle NACHT (domain existing in NAIP, CIITA, HET-E and TP-1) domain, and the C-terminal leucine-rich repeat (LRR) domain.

The TLR3 signaling pathway

When binding dsRNA, TLR3 dimerizes [38,40]. The C-terminal TIR domains of dimeric TLR3 interact with the adaptor TRIF (TIR domain-containing adaptor protein-inducing IFNβ) [41]. TRIF, in turn, recruits Lys63-linked polyubiquitinated TRAF6 (TNF receptor-associated factor 6), thereby leading to the Lys63-linked polyubiquitination of TAK1 (TGF-β activated kinase 1); TAK1 further recruits TAB 1/2/3 (TAK1-binding protein 1/2/3), thus yielding the quaternary TAK1/TAB 1/TAB 2/TAB 3 complex, which activates IKKα/β/γ (IκB kinase alpha, beta and gamma; IKKγ is also known as NEMO, NF-κB essential modulator) [42–45]. Subsequently, the IKKs mediate the phosphorylation and degradation of the NF-

κB inhibitor, IκB. Without IκB binding, NF-κB will enter the nucleus and trigger the expression of inflammatory genes (Fig. 2A).

Also, TRIF can interact with TRAF3 modified by Lys63-linked polyubiquitination, in order to further recruit TBK1 (TANK-binding kinase 1) and IKKε (IκB kinase epsilon) [41,46]. IKKγ (NEMO) is also involved in activating TBK1 and IKKε (Fig. 2A) [47]. The activated TBK1/IKKε will phosphorylate IRF3 [48,49], thereby inducing IRF3 dimerization and nuclear translocation to trigger type-I (mainly IFNβ) and type-III IFN production (Fig. 2A). Subsequently, the expression of IRF7 is upregulated. TBK1/IKKε also phosphorylates IRF7 [49], the activated IRF7 can stimulate the release of various IFNs (Fig. 2A).

The TLR7 signaling pathway

Upon PAMP binding, TLR7 recruits the adaptor MyD88 (myeloid differentiation primary response gene 88) [50]. Next, MyD88 forms a complex with interleukin-1 receptor-associated kinases (IRAKs) (such as IRAK4, IRAK1, and IRAK2) [37,51]. Subsequently, IRAK4 activates IRAK1/2 and then IRAKs dissociate from upstream MyD88 and interact with downstream TRAF6 [51], further activating the NF-κB signaling pathway as described above (Fig. 2A). Meanwhile, multiple proteins, TRAF6, TRAF3, IRAK4, IRAK1, and IKKα can form a complex for signaling. When contacting this complex, IRF7 is phosphorylated by both IRAK1 and IKKα, thus activating the downstream signaling [37,51].

RIG-I-like receptors (RLRs)

Currently, RLRs comprise three cytosolic proteins: RIG-I [52], melanoma differentiation-associated antigen 5 (MDA5) [53], and 'laboratory of genetics and physiology 2' (LGP2) [54]. RIG-I and MDA5 each contain two N-terminal cysteine-aspartic protease (caspase)-recruiting subdomains (CARDs), a central DExD/H helicase domain, as well as the C-terminal repressor domain (RD) (Fig. 3). In contrast, LGP2 lacks the CARDs domain.

The helicase and RD domains of the RLRs are involved in recognizing the dsRNA of RNA viruses [52], while the CARD subdomains lead to intracellular signaling events [31,52]. Due to the absence of CARDs, LGP2 plays a role in regulating RIG-I and MDA5 signaling. Interestingly, LGP2 is a negative regulator of RIG-I signaling [54,55], while it acts a positive regulator facilitating MDA5 binding to viral RNA, thereby augmenting the MDA5 signaling pathway [56,57]. RIG-I preferentially binds short dsRNA (< 1 kb), while MDA5 binds long dsRNA (> 2 kb) [31]. Furthermore, RIG-I is critical for detecting paramyxoviruses, influenza virus, and Japanese encephalitis virus (JEV), whereas MDA5 recognizes mainly picornaviruses as well as HCV [58,59].

When RIG-I binds the PAMPs, the CARDs domain is exposed to interact with the CARD domain of MAVS (mitochondrial antiviral-signaling protein; also known as IPS-1, Cardif, VISA), which is localized to the membrane of mitochondria [60]. Also, MAVS forms oligomers *via* its CARD domain, a process that is necessary for downstream signaling [61]. At the same time, RIG-I binding to MAVS is promoted by ubiquitination through TRIM25 [62]. The RIG-I-MAVS interaction stimulates TRAF3 and TRAF6 [63,64]. Subsequently, the signals are transduced by the downstream complexes TBK1–IKKε and IKKα/β/γ to further induce the activation of the IRF3 and NF-κB pathways, respectively, similarly to the downstream signaling pathway of TLR3 mentioned above (Fig. 2A). Finally, these signals trigger the production of IFNs and other host cytokines.

NOD-like receptors (NLRs)

NOD-like receptors are cytosolic proteins. They are activated in response to PAMPs in the cytosol (Fig. 2A). The members of the NLR family have various domain architectures [65]. However, they contain three common subdomains: (a) the N-terminal effector-binding domain (EFB), for example, a CARD domain, a pyrin domain (PYD), or a baculovirus inhibitor of apoptosis protein repeat (BIR) domain; (b) the middle NACHT domain (exists in NAIP, CIITA, HET-E, and TP-1); (c) the C-terminal LRR domain (Fig. 3). According to the different N-terminal domains, the NLRs are divided into five families: NLRA (N-terminal acidic activation domain), NLRB (N-terminal BIR domain), NLRC (N-terminal CARD domain), NLRP (N-terminal PYD domain), and NLRX (N-terminal unknown domain) [65]. Here, we discuss two well-characterized NLRs, NLRP3 and NLRC2, that regulate host immune responses during viral infection.

NLRP3 is sensitive to infection by several (−) ssRNA and (+)ssRNA viruses, such as influenza A virus (IAV), vesicular stomatitis virus (VSV), encephalomyocarditis virus (EMCV), and HCV [66–68]. When NLRP3 is activated by PAMPs derived from invasive viruses, oligomeric NLRP3s interact with ASC (apoptosis-associated speck-like protein) and procaspase-1 (Fig. 2A). They form an inflammasome complex, which results in the activation of caspase-1,

thus leading to the maturation of pro-IL-1β and pro-IL-18 (Fig. 2A) [36,66–68]. However, so far, there is no evidence for NLRP3 directly binding virus ssRNA or dsRNA. NLRP3 inflammasome activation relies on lysosomal maturation and the production of reactive oxygen species (ROS) during IAV infection [66]; therefore, NLRP3 is likely activated by intracellular changes (such as lysosomal maturation and ROS formation) but not directly by interaction with PAMPs [33,36].

NLRC2 (alternatively named NOD2), as an intracellular innate immune sensor, recognizes bacterial MDP (muramyl dipeptide) to regulate the host immune response [69]. It also recognizes the RNA of several (−)ssRNA viruses, such as IAV, VSV, and respiratory syncytial virus (RSV) [70]. NLRC2 directly interacts with viral ssRNA and recruits MAVS to activate the IRF3 pathway, thereby releasing the type-I IFN, IFNβ [70]. NLRC2 can also activate TRAF6 and stimulate the NF-κB pathway [71].

RNA-virus proteases interfering with the host innate immune response

Viral proteases are not only important for processing the polyproteins in (+)ssRNA viruses but are also involved in counteracting the host innate immune response. In this review, we focus on the viral proteases of three RNA virus families (Picornaviridae, Coronaviridae, and Flaviviridae) and discuss how they antagonize the host's antiviral response.

The 2A and 3C proteases of Picornaviridae

Two viral proteases, the $2A^{pro}$ and the $3C^{pro}$, are required for processing the polyprotein in the viral life cycle [4]. However, several picornaviruses, such as Foot-and-Mouth disease virus (FMDV), have yet another protease, the L^{pro} [4]. Interestingly, hepatitis A virus (HAV) has exclusively the 3C protease [72], whereas the 2A protein is part of the virion [73]. Picornaviruses are detected by RLRs, mainly by MDA5, as well as by TLRs [74,75]. It is no surprise that picornaviruses have evolved efficient ways to inhibit the antiviral type-I IFN production. In particular, the $2A^{pro}$ and the $3C^{pro}$ can disrupt the RLR- or TLR-mediated innate immune pathways. We will discuss further below how the L^{pro} counteracts the host innate immune response.

$2A^{pro}$ antagonizes the host immune response

The members of the genus *Enterovirus* of the Picornaviridae family have been well investigated regarding the mechanism of innate immunity disruption by the $2A^{pro}$ [76–78]. The enteroviral $2A^{pro}$ possesses a Cys–His–Asp catalytic triad [16]. It cleaves between P1 and P2, that is, the site between the capsid and nonstructural-protein precursors, which is an essential event in the enterovirus life cycle [4]. Few inhibitors of the enteroviral $2A^{pro}$, let alone an antiviral drug targeting this enzyme, have been described so far. The peptide LVLQTM was shown to antagonize enterovirus A71 (EV-A71) $2A^{pro}$ through binding to its active site [79].

$2A^{pro}$ cleaves MDA5 and MAVS

The picornavirus $2A^{pro}$ modulates the MDA5–MAVS-mediated antiviral pathway. The Coxsackievirus B3 (CVB3), poliovirus (PV), and EV-A71 $2A^{pro}$s were shown to cleave both MDA5 and MAVS, leading to inhibition of IFNβ and type-III IFN (IFNλ1-4) production (Fig. 2A) [76–78]. Feng *et al*. [77] concluded that enteroviruses use a common strategy to antagonize the host IFN response. Furthermore, these authors found that MDA5 and MAVS were degraded by a caspase-proteasome-independent pathway in CVB3-infected cells. In contrast, Barral *et al*. [80] reported that MDA5 was cleaved *via* the caspase-proteasome-dependent pathway in PV infection.

$2A^{pro}$ cleaves TRIF

TRIF is an important adaptor in the TLR3 pathway [41]. The protein level of TRIF is reduced in CVB3-infected cells due to the $3C^{pro}$ [81] (see below). In 2016, Lind *et al*. [78] found that CVB3 $2A^{pro}$ also cleaves TRIF (Fig. 2A), and further antagonizes type-I and type-III IFN production.

Does the $2A^{pro}$ affect the JAK-STAT pathway?

EV-A71 infection leads to increased IFNβ levels but inhibits the transcription of ISGs *in vivo* [82]. Lu *et al*. [82] found that the $2A^{pro}$ reduces IFNAR1 expression levels to impede the JAK-STAT pathway (Fig. 2B), thereby leading to a decreased production of ISGs. Furthermore, the protease activity of the $2A^{pro}$ was essential for downregulating IFNAR1. However, Liu *et al*. [83] reported that EV-A71 infection did not alter IFNAR1 but instead JAK1 expression *in vivo*. Furthermore, overexpressing viral $2A^{pro}$ (or $3C^{pro}$) did not affect the JAK1 expression level. Conclusively, these authors demonstrated that the $2A^{pro}$ does not act as an antagonist to the JAK-STAT pathway, although EV-A71 infection does affect this signaling pathway by inhibiting JAK1 expression [83]. Very recently, Wang

et al. reported that EV-A71 infection leads to degradation of karyopherin-α1 (KPNA1), a nuclear localization signal receptor for phosphorylated STAT1. Thus, STAT1 transport into the nucleus is blocked, thereby shutting off the JAK-STAT pathway [84]. Interestingly, these authors found that neither the $2A^{pro}$ nor the $3C^{pro}$ is the culprit here; instead, it is caspase-3 activated by the virus infection that degrades KPNA1 [84]. However, it is still unclear whether $2A^{pro}$ can affect the JAK-STAT pathway by other mechanisms or does not affect this signaling pathway at all.

Finally, the $2A^{pro}$ can degrade PABP (poly(A)-binding protein) and eIF4G (eukaryotic initiation factor 4G) to shut down the host translation machinery [85–87], thereby globally inhibiting the production of antiviral host proteins.

$3C^{pro}$ antagonizes the host immune response

The $3C^{pro}$ has either a catalytic Cys–His dyad or a Cys–His–Asp/Glu triad in different picornaviruses (Fig. 1B) [17–19]. The protease prefers to cleave between Gln and Gly (and sometimes, between Glu and Gly) [88]. Besides viral polyprotein processing, this protease also has an RNA-binding activity being essential for viral RNA replication [89]. Currently, Michael-acceptor compounds such as rupintrivir and SG85 have been described as potent, broad-spectrum inhibitors of enterovirus 3C proteases [19,90,91].

$3C^{pro}$ modulates RIG-I, MDA5, and MAVS

The picornavirus $3C^{pro}$ inhibits the RLR signaling pathway. EV-A71 $3C^{pro}$ has been reported to bind the N-terminal CARDs of RIG-I without digesting RIG-I, thereby inhibiting the recruitment of MAVS and disrupting the type-I IFN response [92]. At variance with this report, Feng *et al*. [77] found that not only the EV-A71 enzyme but also the CVB3 and PV $3C^{pro}$s do cleave RIG-I *in vivo*. EMCV $3C^{pro}$ can cleave RIG-I *in vitro* [93]. A caspase-mediated degradation of RIG-I was also observed in EMCV-infected cells [93]. The exact mechanism of the RIG-I regulation by $3C^{pro}$ needs to be further investigated; in any case, the partly conflicting observations mentioned above indicate that RIG-I is an important target antagonized by the picornavirus $3C^{pro}$.

Like RIG-I, MDA5 binds MAVS to activate downstream cascades of the innate immune system (see above). Lei *et al*. [92] found by co-immunoprecipitation (co-IP) that EV-A71 $3C^{pro}$ can bind MDA5 (Fig. 2A). Furthermore, Rui *et al*. [94] detected by co-IP that the CV-A16, CV-A6, or EV-D68 $3C^{pro}$s can also bind MDA5, thus disrupting the MDA5–MAVS interaction. Interestingly, these $3C^{pro}$s do not digest MDA5 and a proteolytically inactive, mutated $3C^{pro}$ can also prevent MDA5 from activating IFN.

Differently, HAV can cleave MAVS through the 3ABC precursor protein [the 3A (a membrane anchor protein), 3B (VPg) plus protease domain] but not through the mature $3C^{pro}$ alone [95]. Mukherjee *et al*. [81] demonstrated that MAVS was cleaved between Gln148 and Ala149 by the $3C^{pro}$ in CVB3-infected cells. Recently, the picornavirus Seneca Valley virus (SVV) $3C^{pro}$ was also shown to induce cleavage of MAVS at the same position, Gln148↓Ala149 (↓: cleavage site) [96]. Therefore, both viruses suppress the antiviral IFN production through cleavage of MAVS.

$3C^{pro}$ cleaves TRIF

The picornavirus $3C^{pro}$ can also interfere with the TLR3 pathway. As mentioned above, the C-terminal TIR domains of dimeric TLR3 interact with TRIF to stimulate the downstream IRF3 and NF-κB activities. CVB3 $3C^{pro}$ was demonstrated to cleave TRIF (Fig. 2A), thereby blocking the downstream type-I IFN production in CVB3-infected cells [81]. In total, five cleavage sites in TRIF (Gln190↓Gly191, Gln653↓Ser654, Gln659↓Ser660, Gln672↓Ser673, and Gln702↓Ala703) were found [81]. Furthermore, the $3C^{pro}$ of EV-A71 or EV-D68 can also cleave TRIF, leading to inactivation of the signaling along the IRF3 and NF-κB pathways *in vivo* [97,98]. However, the EV-A71 $3C^{pro}$ processes only one site between Gln312 and Ser313, while the EV-D68 protease cleaves two sites (Gln312↓Ser313, Gln653↓Ser654) [97,98]. It seems that the different $3C^{pro}$s possess slightly different cleavage patterns on TRIF. Whether these subtleties are linked to any difference in biological response needs to be answered. Similarly to the 3ABC precursor digesting MAVS (see above), the HAV protease can also cleave TRIF *in vivo* [99], but the degradation appears to be exclusively performed by the 3CD (protease-polymerase precursor) protein, not by mature 3C protease alone. The two cleavage sites in TRIF are Gln190↓Gly191 and Gln554↓His555 [99]. The observation that some precursor proteins (such as HAV 3ABC, 3CD) seem to be involved in counteracting the host immune response should motivate further investigations into more protease precursors, instead of looking only into mature proteases.

$3C^{pro}$ cleaves IKKγ (also named NEMO)

The FMDV $3C^{pro}$ can process the porcine IKKγ (also called NEMO) at the unusual cleavage site Gln384↓Arg385, thereby removing the C-terminal zinc-

finger domain of this protein [100] (these authors erroneously misnumbered Gln384 as Gln383), thus blocking the signaling pathways of NF-κB and IRF3. From the same group, Wang *et al.* [101] reported that mature HAV $3C^{pro}$ can cleave NEMO at position Gln304↓Ala305, thereby antagonizing type-I IFN production. These authors also reported that the precursor proteins 3ABC or 3CD of HAV can also cleave NEMO but with less efficiency [101].

$3C^{pro}$ cleaves TANK

TANK (TRAF family member-associated NF-κB activator), as a positive regulator, interacts with the TBK1/IKKε complex to enhance type-I IFN production [102]. However, the role of TANK in regulating the NF-κB pathway is a matter of debate. Chariot *et al.* [103] reported that TANK binds IKKγ (NEMO) and upregulates the NF-κB pathway. Blocking the TANK–IKKγ interaction by deleting the TANK-binding domain of IKKγ impairs NF-κB activation [103]. However, Lys63-linked polyubiquitination of TRAF6 is required for NF-κB activation [104]. Wang *et al.* [105] proposed that TANK acts as a negative regulator of the NF-κB pathway by inducing TRAF6 deubiquitination.

The EMCV $3C^{pro}$ can cleave TANK at two sites, Gln197↓Ala198 and Gln291↓Gly292 [106]. Huang *et al.* [106] reported that NF-κB signaling increased when TANK was processed by EMCV $3C^{pro}$. According to Wang *et al.*'s proposal [105] (see above), the explanation might be that the degradation of TANK can release TANK–TRAF6-mediated NF-κB inhibition. From the same group, Huang *et al.* [107] reported that the EMCV $3C^{pro}$ can disrupt the TANK–TBK1–IKKε–IRF3 complex by cleaving TANK, thus decreasing type-I IFN production. It is of interest to further investigate the reason why the EMCV $3C^{pro}$ processes TANK to stimulate the NF-κB pathway but downregulate the IRF3 pathway. Very recently, Qian *et al.* [96] showed that the SVV $3C^{pro}$ processes TANK at two cleavage sites, Glu272↓Phe273 and Gln291↓Gly292. Whereas the former site is unusual because of the large P1' residue, the latter is also cleaved by the EMCV $3C^{pro}$, indicating that it may be a conserved target on TANK for different picornavirus $3C^{pro}$s.

$3C^{pro}$ cleaves TAK1/TAB 1/TAB 2/TAB 3

The EV-A71 $3C^{pro}$ uses another mechanism to deactivate the NF-κB pathway. As mentioned above, TAK1 can bind TAB 1 to form a complex [42]. This complex recruits TAB 2 and TAB 3, yielding the quaternary TAK1/TAB 1/TAB 2/TAB 3 [43,44]. The combination of TAK1 and TABs can activate IKKs (such as IKKα, IKKβ, and IKKγ) [45], thereby upregulating the NF-κB pathway. The EV-A71 $3C^{pro}$ cleaves TAK1 (Gln360↓Ser361), TAB 1 (Gln414↓Gly415 and Gln451↓Ser452), TAB 2 (Gln113↓Ser114), and TAB 3 (Gln173↓Gly174 and Gln343↓Gly344) *in vivo* (Fig. 2A) [108]. Recently, the CV-A16, CV-A6, and EV-D68 $3C^{pro}$s have also been shown to process TAK1 [94]. In summary, the enterovirus $3C^{pro}$ impairs NF-κB activation.

$3C^{pro}$ cleaves IRFs

IRF7 stimulates type-I IFN production, such as IFNα, thereby activating the JAK-STAT pathway in adjacent cells [109]. The $3C^{pro}$ of EV-A71 can process IRF7 at a cleavage site between Gln189 and Ser190 *in vitro* and *in vivo*, while the $3C^{pro}$ of EV-D68 does so at two sites (Gln167↓Ala168 and Gln180↓S190) [110,111].

Furthermore, IRF9 interacts with STAT1 and STAT2 to form a complex, ISGF3 in the JAK-STAT pathway, thereby stimulating ISG production (Fig. 2B) [30,112]. The EV-A71 $3C^{pro}$ can cleave IRF9 in EV-A71-infected cells as well as in an *in vitro* assay, resulting in reduced IFN signaling [113].

Finally, the $3C^{pro}$ can digest PABP to shut off host translation [114,115], thereby globally inhibiting the production of antiviral proteins.

L^{pro} interferes with the host innate immune response

So far, the roles of the L^{pro} have been well investigated for FMDV. Due to initiation at different AUG codons, two forms of the L^{pro}, Lab^{pro} and Lb^{pro}, were discovered in FMDV [116]. The FMDV L^{pro}, a papain-like protease, contains a Cys–His catalytic dyad [25].

The FMDV L^{pro} can degrade p65/RelA, a subunit of NF-κB, to block the NF-κB activity [117]. de los Santos *et al.* [118] found that a putative SAP (SAF-ACINUS-PIAS) domain of the L^{pro} affects its subcellular localization, thus further mediating the degradation of p65/RelA. Also, the FMDV L^{pro} can decrease the IRF3 and IFR7 protein levels *in vivo* [119], but the corresponding mRNAs are apparently not affected.

Medina *et al.* [120] recently reported that the FMDV L^{pro} binds the host transcription factor ADNP (activity-dependent neuroprotective protein) *in vitro* and *in vivo*. In addition, these authors found that wild-type FMDV but not ΔL^{pro} FMDV can induce ADNP to bind to IFNα promoter sites (IPS; Fig. 2A), thus disrupting the expression of IFN and ISGs [120].

Furthermore, the FMDV Lb^{pro} exhibits deubiquitinating activity [121]; it can remove Lys48- and Lys63-linked polyubiquitin *in vitro* and *in vivo*. As mentioned above, the ubiquitination of several elements is essential in innate immune pathways, for example, of RIG-I, TRAF3, and TRAF6 [62,104,122]. Wang *et al*. [121] reported that the FMDV Lb^{pro} can deubiquitinate RIG-I, TBK1, TRAF3, and TRAF6 in HEK293T cells overexpressing this protease, which leads to blocking type-I IFN production.

Like the $2A^{pro}$, the L^{pro} can also cleave eIF4G to globally inhibit the translation of mRNAs coding for host antiviral proteins [25,87].

Many investigations have shown that the papain-like proteases of coronaviruses also possess DUB activity relevant for antagonizing the host innate immune response; these enzymes are discussed in the next paragraph.

Papain-like proteases and 3C-like proteases of the Coronaviridae interfere with innate immunity

Belonging to the family Coronaviridae, coronaviruses have one or two viral PL^{pro}(s) and one $3CL^{pro}$ (M^{pro}) [9]. The PL^{pro}(s) is (are) part of the nonstructural protein 3 (Nsp3) [123,124]. PL^{pro} is a cysteine protease with a catalytic triad Cys–His–Asp (Fig. 1B) [26]. The CoV PL^{pro} has proteolytic, deubiquitinating, and deISGylating (removal of ISG15 from target proteins) activities [26,27,125]; through the latter two, it can disrupt the host immune response. Thus far, only a few inhibitors targeting the PL^{pro} have been described. Báez-Santos *et al*. [126] demonstrated that several naphthalene derivatives efficiently block the enzymatic activity of SARS-CoV PL^{pro}.

PL^{pro} modulates the TLR7 pathway by deubiquitinating TRAF3 and TRAF6

As mentioned above, TLR7 recognizes ssRNA [33,37]. In 2013, Li *et al*. [127] showed that GU-rich ssRNA of SARS-CoV can be detected by TLR7.

The SARS-CoV PL^{pro} removes Lys63-linked ubiquitin (Ub) chains from TRAF3 and TRAF6 to reduce the TLR7-mediated immune signaling [128]. Furthermore, the SARS-CoV PL^{pro} cannot remove Lys48-linked Ub chains from TRAF3 and TRAF6 according to a western blot assay [128]. This is at variance with an *in vitro* study that demonstrated that SARS-CoV PL^{pro} prefers to process Lys48- over Lys63-linked polyUb chains [129]. Perhaps, one might speculate that the target proteins, TRAF3 or TRAF6, affect the PL^{pro} DUB specificity.

In addition, TRAF3 and TRAF6 are two key components of the RLR pathways (Fig. 2A); therefore, we have reason to believe that PL^{pro} could also regulate RLR signaling by deubiquitinating these two targets.

PL^{pro} modulates the STING–TRAF3–TBK1–IKKε complex

STING (stimulator of IFN genes, also known as MITA, ERIS) is a protein of the endoplasmic-reticulum (ER) (Fig. 2A). It can activate the IRF3 pathway upon dimerization and ubiquitination as well as upon interaction with several partners, such as MAVS, TRAF3, TBK1, and IKKε [130,131]. The SARS-CoV PL^{pro}+TM (TM: transmembrane region of Nsp3; see Ref. [124] for a review) and Human Coronavirus-NL63 (HCoV-NL63) $PL2^{pro}$+TM bind STING in a co-IP assay [132]. These two proteins inhibit the dimerization and ubiquitination of STING and disrupt STING interaction with other partners, thereby blocking STING-mediated IFN production. Interestingly, the enzymatic activity of SARS-CoV PL^{pro}+TM or HCoV-NL63 $PL2^{pro}$+TM is not required for modulating STING [132].

Furthermore, SARS-CoV PL^{pro}+TM can disrupt the STING–TRAF3–TBK1–IKKε complex by binding each of its components [133]. In addition, the SARS-CoV PL^{pro}+TM or PL^{pro} alone were also reported to bind IRF3 [133,134]. Meanwhile, SARS-CoV PL^{pro} reduces the ubiquitination of STING, TRAF3, and TBK1 [133]. Also, murine hepatitis virus A59 (MHV-A59) $PL2^{pro}$ deubiquitinates TBK1 and binds TBK1 and IRF3 [135,136]. All these observations demonstrate that the PL^{pro} is heavily involved in regulating the IRF3 pathway.

PL^{pro} blocks the p53–IRF7–IFNβ pathway

The tumor suppressor protein p53 enhances the antiviral type-I IFN response [137]. In 2015, Yuan *et al*. [138] found that p53 can upregulate the transcription of IRF7. HCoV-NL63 $PL2^{pro}$ deubiquitinates and stabilizes MDM2, a p53 degradation stimulator, thus causing p53 degradation and blocking the p53–IRF7–IFNβ signaling pathway (Fig. 2A) [138]. p53 also inhibits SARS-CoV replication [139]. Ma-Lauer *et al*. [139] found that the PL^{pro}s of SARS-CoV and MERS-CoV as well as the two PL^{pro}s of HCoV NL63 can bind RCHY1, another p53-degradation stimulator. The SARS-CoV 'unique domain' (SUD) enhances the interaction between the PL^{pro} and RCHY1. This interaction increases the stability of RCHY1, thereby stimulating p53 degradation [139]. In conclusion, the coronavirus

PL^{pro} utilizes various ways to modulate p53 and further regulate host innate immunity responses.

PL^{pro} blocks the NF-κB pathway

Besides blocking the IRF3 pathway, Frieman *et al.* [140] reported that the SARS-CoV PL^{pro} stabilizes IκBα, an inhibitor of NF-κB, to modulate the NF-κB signaling pathway. Further, these workers found that the HCoV-NL63 but not the MHV $PL2^{pro}$ can counteract the IRF3 and NF-κB pathways [140]. These observations indicate that the functions of the PL^{pro} could be specific for different CoVs.

Furthermore, Devaraj *et al.* [134] indicated that the protease activity of the SARS-CoV PL^{pro} is not required for blocking IFNβ production. Frieman *et al.* [140] reported that the enzyme activity of SARS-CoV PL^{pro} is dispensable for IFNβ production *via* the IRF3 pathway but not for TNFα production through the NF-κB pathway. In 2010, Clementz *et al.* [141] also found that the catalytic activity of the HCoV-NL63 $PL2^{pro}$ is not responsible for blocking IFNβ production. In contrast, the MHV $PL2^{pro}$ requires the enzymatic activity for blocking IFNβ induction [136]. The exact relationship between the enzymatic activity of the PL^{pro} and IFN production is still a matter of debate today.

Other roles of the PL^{pro} in counteracting host immunity

The PL^{pro} has deISG15ylating activity (Fig. 2B) [125], leading to the downregulation of the host immune response. However, the detailed mechanism of this process is still not completely clear. In addition, autophagy could play a negative role in the host innate immune response [142]. Chen *et al.* [143] found that the PL^{pro}+TM of SARS-CoV induces incomplete autophagy by interacting with LC3 and Beclin1 (two key autophagy regulators), thus negatively regulating antiviral immunity. Knockdown of Beclin1 could partially reverse the effect of the PL^{pro} on innate immune signaling [143]. Therefore, these authors assume that the PL^{pro}+TM inducing autophagy could represent a new mechanism of antagonism to host innate immunity by coronaviruses.

$3CL^{pro}$ antagonizes host immune responses

The $3CL^{pro}$ (M^{pro}), the other protease of coronaviruses, is also involved in counteracting the host innate immune response. A number of peptidic and peptidomimetic inhibitors carrying various warheads have been described to block the activity of the coronavirus M^{pro} ([144]; see Refs [9,145] for reviews).

The M^{pro}s of two CoVs infecting pigs have recently been reported to antagonize the host immune response (Fig. 2) [146–148]. The M^{pro}s of both porcine epidemic diarrhea virus (PEDV, a member of the genus *Alphacoronavirus*) and porcine deltacoronavirus (PDCoV) cleave porcine IKKγ (NEMO) at the identical site, Gln231↓Val232 [146,147]. As mentioned above, NEMO is required for activating the NF-κB and IRF3 pathways. Therefore, the cleavage of IKKγ by PEDV and PDCoV M^{pro}s abrogates NF-κB signaling and inhibits IFNβ induction [146,147]. In addition, the M^{pro} of PDCoV can process porcine STAT2 at two sites, Gln685↓Glu686 and Gln758↓Ser759, to impair the JAK-STAT pathway [148], thereby reducing ISG production. It is interesting to investigate whether the human CoV M^{pro} exhibits similar activities to affect the host innate immune response.

Proteases of Flaviviridae interfering with the innate immune response

In the following paragraphs, we will discuss the proteases of the genera *Hepacivirus*, *Flavivirus*, and *Pestivirus* of the Flaviviridae family.

HCV NS3/NS4A protease counteracts host innate immune pathways

The best known member of the genus *Hepacivirus* is HCV. HCV produces two proteases, $NS2^{pro}$ and $NS3/NS4A^{pro}$ [10,11]. The autoprotease $NS2^{pro}$ operates only on one cleavage site, between NS2 and NS3, while the other cleavage sites among the NS proteins of HCV are processed by the $NS3/NS4A^{pro}$ [11]. Currently, the $NS3/NS4A^{pro}$, but not the $NS2^{pro}$, is reported to be related to counteracting host innate immune responses (Fig. 2A). The former enzyme features the catalytic triad Ser–His–Asp [20]. The cleavage site specificity of the $NS3/NS4A^{pro}$ favors Cys or Thr in the P1 position, an acidic residue in the P6 position, and a residue with a small side-chain (Ala or Ser) in P1′, that is, D/E-XXXX-C/T-S/A for the P6-P1′ sequence [11]. NS4A is a cofactor for the NS3 protease. Several synthetic inhibitors of the HCV $NS3/NS4A^{pro}$, such as simeprevir and paritaprevir (ABT-450), have helped to dramatically improve the therapy of liver disease caused by HCV [149,150].

HCV $NS3/NS4A^{pro}$ cleaves MAVS

In 2005, RIG-I was shown to detect the 3′ UTR (untranslated region) of the HCV genome [151]. However, later Cao *et al.* [59] demonstrated that MDA5 plays a

major role in recognizing the 3′ UTR of HCV while RIG-I seems to be less important. Subsequently, MDA5 (or RIG-I) binds MAVS, thereby activating the downstream IRF3 and NF-κB pathways. HCV NS3/NS4A^{pro} cleaves MAVS (also named Cardif, as mentioned above; Fig. 2A) at the cleavage site Cys508↓His509 [152], thereby disrupting the host immune response. The NS3/NS4A^{pro} of GB virus B (GBV-B), from the same genus as HCV, cleaves MAVS at the same site as the HCV enzyme [153]. These authors further found that MAVS was released from the mitochondrial membrane to the cytosol due to this cleavage [153]. Because the location of MAVS on the mitochondrial membrane is essential for its functions, this observation could explain how MAVS fails to transmit the signal downstream after being processed by NS3/NS4A^{pro} [153]. Furthermore, NS3/NS4A proteases from Hepaciviruses infecting other animals (such as monkeys, rodents, horses, and cows) can cleave their cognate MAVS proteins [154]. The cleavage of MAVS presents a common mechanism used by Hepaciviruses to regulate the host immune response.

NS3/NS4A^{pro} cleaves Riplet (upstream regulator of RIG-I)

As mentioned above, RIG-I is ubiquitinated by TRIM25 for its activation [62]. Oshiumi *et al.* [155] reported that the protein Riplet (an E3 ubiquitin ligase) is a prerequisite for TRIM25 stimulation of RIG-I signaling. Knocking out Riplet abrogates the expression of type-I IFN in response to HCV RNA [155]. HCV NS3/NS4A^{pro} can cleave Riplet at position Cys21↓Ile22 *in vitro*, because the residues 16-EDDLGC-21 of Riplet are similar to the consensus cleavage motif D/E-XXXX-C/T of HCV NS3/NS4A protease. As a consequence, RIG-I activation is abolished [155].

NS3/NS4A^{pro} modulates TRIF of the TLR3 pathway

TLR3 is sensitive to the intermediate dsRNA of HCV replication [156]. Upon sensitization, its C-terminal TIR domain can interact with TRIF to stimulate the downstream cascades. HCV NS3/NS4A^{pro} cleaves TRIF at the site Cys372↓Ser373 *in vitro* and *in vivo* (HEK293 cells) to disrupt the TLR3 pathway [157]. In contrast to this observation, Dansako *et al.* [158] found that HCV NS3/NS4A cannot cleave TRIF in PH5CH8 (immortalized human hepatocytes), HeLa, and Huh-7-derived cells. The effects of the NS3/NS4A protease on TRIF need to be further investigated, in order to resolve this ambiguity.

NS3/NS4A^{pro} modulates importin β1

Very recently, Gagné *et al.* [159] found that the HCV NS3/NS4A^{pro} can cleave importin β1 (IMPβ1; Fig. 2A). IMPβ1, a nucleocytoplasmic transport receptor, transports proteins from the cytoplasm to the nucleus. The HCV NS3/NS4A protease triggers the degradation of IMPβ1 and inhibits or disrupts the nucleocytoplasmic trafficking of IRF3 as well as NF-κB p65, thus preventing the host immune response [159].

Flavivirus NS2B/NS3 proteases counteracting host innate immune pathways

Flaviviruses only have one protease, the NS2B/NS3^{pro} [12]. This enzyme comprises the N-terminal third of NS3 and the middle hydrophilic part of NS2B as a cofactor, together forming the NS2B/NS3^{pro}. Like HCV NS3/NS4A^{pro}, the flavivirus NS2B/NS3^{pro} is a chymotrypsin-like serine protease with a catalytic Ser–His–Asp triad (Fig. 1B) [21,22]. The P1 and P2 positions at the NS2B/NS3^{pro} cleavage sites are conserved as basic residues, Lys or Arg. The NS2B/NS3^{pro} is an attractive antiviral target. This protease is also involved in counteracting host innate immune pathways (Fig. 2A). Currently, no approved drug is available that targets the flavivirus NS2B/NS3^{pro}. Several peptide aldehydes and peptide boronic-acid inhibitors have been described to inhibit the activity of the flavivirus NS2B/NS3^{pro} [22,160–162].

The NS2B/NS3^{pro} cleaves STING

As mentioned above, STING can upregulate IRF3 signaling (Fig. 2A) [130,131]. DENV NS2B/NS3^{pro} cleaves human STING at the site Arg94-Arg95↓Gly96 *in vivo* and thereby inhibits induction of IFNβ [163,164]. However, this protease is unable to cleave RIG-I, TLR3, TBK1, IKKε, IRF3, and IRF7 [163]. Recently, Liu *et al.* [165] reported that the full-length DENV NS3 (including the C-terminal helicase), but not the NS2B, can be modified by Lys27-linked polyubiquitination when co-transfecting Ub and NS3 in HEK 293T cells. The ubiquitinated NS3 facilitates recruitment of NS2B, that is, the formation of the NS2B/NS3 protease, thereby enhancing the cleavage of STING. Furthermore, these authors found that the ER protein SCAP (sterol regulatory element-binding protein (SREBP) cleavage-activating protein) can bind NS2B and inhibit polyubiquitination of NS3, thus disrupting the formation of NS2B/NS3^{pro} and the cleavage of STING [165].

The NS2B/NS3 protease cleaves two mitofusins (MFN1, MFN2)

MFN1 and MFN2 regulate the mitochondrial fusion; in particular, MFN1 is required for the RLR signaling pathway [166]. Yu *et al*. [167] demonstrated that the DENV NS2B/NS3 protease can cleave MFN1 (Arg539-Asn540↓Ala541) and MFN2 (Arg563-Arg564↓Ala565) in cells. Subsequently, the cleaved MFNs suppress mitochondrial fusion and disrupt IFN production. Interestingly, the homologous protease from JEV cannot cleave MFNs for unknown reasons [167]. It is worth investigating whether or not other flavivirus proteases modulate MFNs.

Pestivirus N-terminal protease counteracts host immune responses

As mentioned above, a total of three proteases – N^{pro}, $NS2^{pro}$, and $NS3/NS4A^{pro}$ – are encoded by the pestivirus genome. To our knowledge, only the N^{pro} is reported to be involved in counteracting the host innate immune pathways (Fig. 2A); therefore, we will restrict ourselves to discussing this enzyme here. The pestivirus N^{pro} is cleaved off the polyprotein by autolysis between C (the capsid protein) and the N^{pro} [14]. It is a cysteine protease with a catalytic dyad Cys–His. The N^{pro} adopts neither a chymotrypsin-like nor a papain-like fold. Instead, it features a unique 'clam-like' fold containing a catalytic protease domain and a zinc-binding domain [168]. After autocleavage, the N^{pro} loses its cleavage capability by intramolecular auto-inhibition [168].

N^{pro} binds IRF3 and IRF7

The N^{pro}s of CSFV and BVDV directly bind IRF3 and induce degradation of the factor by the host proteasome, thus interfering with IFN production [169–172]. According to point mutation experiments, both the protease domain and the zinc-binding domain are essential for N^{pro} binding to IRF3 [168,173,174].

Furthermore, the CSFV N^{pro} can also bind IRF7 and downregulate the IRF7 protein level in porcine DC cells, thus limiting type-I IFN production [175]. Also, Fiebach *et al*. [175] found that the zinc-binding domain but not the protease domain is required to bind IRF7.

N^{pro} interacts with IκBα (NF-κB inhibitor)

The CSFV N^{pro} binds IκBα *in vitro* and *in vivo* [176]. However, the enzyme does not affect the NF-κB activity [176]. The BVDV N^{pro} cannot block the NF-κB pathway either [171]. The role of the N^{pro}-IκBα interaction, thus, remains unclear for the time being.

Conclusions

The proteases of emerging or re-emerging (+)ssRNA viruses are always worth investigating, either as targets for direct antivirals disrupting polyprotein processing [9,162,177] or as important players in mounting the viral anti-IFN activity. In this review, we discussed the roles of viral proteases from the families Picornaviridae, Coronaviridae, and Flaviviridae in counteracting host innate immune responses. Among the different PRR-mediated signaling pathways, a large body of data is available for components of the RLR and TLR pathways being cleaved by viral proteases, but much less so for the NLR pathway (with the notable exception of MAVS in the NLRC2 pathway as a prominent target of viral proteases). A possible reason for this could be that at this time, many immunity-related functional roles of NLRs remain unclear. Another observation is that a multitude of reports exist on the proteolytic cleavage of components of the innate immune system by the picornaviral $2A^{pro}$ and $3C^{pro}$ as well as the HCV $NS3/NS4A^{pro}$, while proteolytic cleavage by the coronavirus proteases PL^{pro} and $3CL^{pro}$ (M^{pro}) seems to be comparatively rare. This may be due to more research having been performed on the picornaviruses and on HCV, or to the fact that the DUB activity of the coronavirus PL^{pro} (as opposed to its proteolytic activity) is a very efficient player in counteracting the innate immune response. Furthermore, it should be remembered that CoVs feature many other proteins (such as ORF3b, ORF6, the nucleocapsid protein, the membrane protein, and the X domain in SARS-CoV; ORF4a, ORF4b, ORF5, and the membrane protein in MERS-CoV) that are involved in suppressing IFN production [124,178], so proteolytic cleavage of host immunity proteins is perhaps required to a lesser extent here. For picornaviruses and HCV on the other hand, there is only occasional reports on non-proteases, such as the picornaviral 2C and 3A proteins [179,180] as well as HCV NS5A and E2 [181,182], being involved in diminishing cytokine production.

In general, homologous proteases from the same family show common mechanisms in regulating host immunity pathways. For example, all $3C^{pro}$s from CVB3, EV-A71, and SSV cleave TRIF. However, occasionally homologous enzymes exhibit some unique characteristics; thus, the DENV but not the JEV NS2B/NS3 protease can cleave MFNs. All these findings not only contribute to our understanding of the host's immune response to viral infection but can also

help us discover broad-spectrum or specific antiviral drugs targeting viral proteases and their interaction with host signaling pathways.

References

1 Adams MJ, Lefkowitz EJ, King AMQ, Harrach B, Harrison RL, Knowles NJ, Kropinski AM, Krupovic M, Kuhn JH, Mushegian AR *et al.* (2017) Changes to taxonomy and the International Code of Virus Classification and Nomenclature ratified by the International Committee on Taxonomy of Viruses. *Arch Virol* **162**, 2505–2538.

2 Jiang P, Liu Y, Ma HC, Paul AV and Wimmer E (2014) Picornavirus morphogenesis. *Microbiol Mol Biol Rev* **78**, 418–437.

3 Norder H, De Palma AM, Selisko B, Costenaro L, Papageorgiou N, Arnan C, Coutard B, Lantez V, De Lamballerie X, Baronti C *et al.* (2011) Picornavirus non-structural proteins as targets for new anti-virals with broad activity. *Antiviral Res* **89**, 204–218.

4 Seipelt J, Guarné A, Bergmann E, James M, Sommergruber W, Fita I and Skern T (1999) The structures of picornaviral proteinases. *Virus Res* **62**, 159–168.

5 Eckerle I, Müller MA, Kallies S, Gotthardt DN and Drosten C (2013) In-vitro renal epithelial cell infection reveals a viral kidney tropism as a potential mechanism for acute renal failure during Middle East Respiratory Syndrome (MERS) Coronavirus infection. *Virol J* **10**, 359.

6 Brierley I, Digard P and Inglis SC (1989) Characterization of an efficient coronavirus ribosomal frameshifting signal: requirement for an RNA pseudoknot. *Cell* **57**, 537–547.

7 Neuman BW and Buchmeier MJ (2016) Supramolecular architecture of the coronavirus particle. *Adv Virus Res* **96**, 1–27.

8 Liu DX, Fung TS, Chong KK, Shukla A and Hilgenfeld R (2014) Accessory proteins of SARS-CoV and other coronaviruses. *Antiviral Res* **109**, 97–109.

9 Hilgenfeld R (2014) From SARS to MERS: crystallographic studies on coronaviral proteases enable antiviral drug design. *FEBS J* **281**, 4085–4096.

10 Grakoui A, McCourt DW, Wychowski C, Feinstone SM and Rice CM (1993) A second hepatitis C virus-encoded proteinase. *Proc Natl Acad Sci USA* **90**, 10583–10587.

11 Bartenschlager R, Ahlborn-Laake L, Yasargil K, Mous J and Jacobsen H (1995) Substrate determinants for cleavage in *cis* and in *trans* by the hepatitis C virus NS3 proteinase. *J Virol* **69**, 198–205.

12 Falgout B, Pethel M, Zhang YM and Lai CJ (1991) Both nonstructural proteins NS2B and NS3 are required for the proteolytic processing of dengue virus nonstructural proteins. *J Virol* **65**, 2467–2475.

13 Rümenapf T, Stark R, Heimann M and Thiel HJ (1998) N-terminal protease of pestiviruses: identification of putative catalytic residues by site-directed mutagenesis. *J Virol* **72**, 2544–2547.

14 Lackner T, Müller A, Pankraz A, Becher P, Thiel HJ, Gorbalenya AE and Tautz N (2004) Temporal modulation of an autoprotease is crucial for replication and pathogenicity of an RNA virus. *J Virol* **78**, 10765–10775.

15 Tautz N, Elbers K, Stoll D, Meyers G and Thiel HJ (1997) Serine protease of pestiviruses: determination of cleavage sites. *J Virol* **71**, 5415–5422.

16 Petersen JF, Cherney MM, Liebig HD, Skern T, Kuechler E and James MN (1999) The structure of the 2A proteinase from a common cold virus: a proteinase responsible for the shut-off of host-cell protein synthesis. *EMBO J* **18**, 5463–5475.

17 Matthews DA, Smith WW, Ferre RA, Condon B, Budahazi G, Sisson W, Villafranca JE, Janson CA, McElroy HE, Gribskov CL *et al.* (1994) Structure of human rhinovirus 3C protease reveals a trypsin-like polypeptide fold, RNA-binding site, and means for cleaving precursor polyprotein. *Cell* **77**, 761–771.

18 Wang J, Fan T, Yao X, Wu Z, Guo L, Lei X, Wang J, Wang M, Jin Q and Cui S (2011) Crystal structures of enterovirus 71 3C protease complexed with rupintrivir reveal the roles of catalytically important residues. *J Virol* **85**, 10021–10030.

19 Tan J, George S, Kusov Y, Perbandt M, Anemüller S, Mesters JR, Norder H, Coutard B, Lacroix C, Leyssen P *et al.* (2013) 3C protease of enterovirus 68: structure-based design of Michael acceptor inhibitors and their broad-spectrum antiviral effects against picornaviruses. *J Virol* **87**, 4339–4351.

20 Kim JL, Morgenstern KA, Lin C, Fox T, Dwyer MD, Landro JA, Chambers SP, Markland W, Lepre CA, O'Malley ET *et al.* (1996) Crystal structure of the hepatitis C virus NS3 protease domain complexed with a synthetic NS4A cofactor peptide. *Cell* **87**, 343–355.

21 Erbel P, Schiering N, D'Arcy A, Renatus M, Kroemer M, Lim SP, Yin Z, Keller TH, Vasudevan SG and Hommel U (2006) Structural basis for the activation of flaviviral NS3 proteases from dengue and West Nile virus. *Nat Struct Mol Biol* **13**, 372–373.

22 Lei J, Hansen G, Nitsche C, Klein CD, Zhang L and Hilgenfeld R (2016) Crystal structure of Zika virus NS2B-NS3 protease in complex with a boronate inhibitor. *Science* **353**, 503–505.

23 Dubrau D, Tortorici MA, Rey FA and Tautz N (2017) A positive-strand RNA virus uses alternative protein-protein interactions within a viral protease/cofactor complex to switch between RNA replication and virion morphogenesis. *PLoS Pathog* **13**, e1006134.

24 Anand K, Palm GJ, Mesters JR, Siddell SG, Ziebuhr J and Hilgenfeld R (2002) Structure of coronavirus main proteinase reveals combination of a chymotrypsin fold with an extra α-helical domain. *EMBO J* **21**, 3213–3224.
25 Guarné A, Tormo J, Kirchweger R, Pfistermueller D, Fita I and Skern T (1998) Structure of the foot-and-mouth disease virus leader protease: a papain-like fold adapted for self-processing and eIF4G recognition. *EMBO J* **17**, 7469–7479.
26 Lei J, Mesters JR, Drosten C, Anemüller S, Ma Q and Hilgenfeld R (2014) Crystal structure of the papain-like protease of MERS coronavirus reveals unusual, potentially druggable active-site features. *Antiviral Res* **109**, 72–82.
27 Lei J and Hilgenfeld R (2016) Structural and mutational analysis of the interaction between the Middle-East respiratory syndrome coronavirus (MERS-CoV) papain-like protease and human ubiquitin. *Virol Sin* **31**, 288–299.
28 Asselin-Paturel C and Trinchieri G (2005) Production of type I interferons: plasmacytoid dendritic cells and beyond. *J Exp Med* **202**, 461–465.
29 Lazear HM, Nice TJ and Diamond MS (2015) Interferon-λ: immune functions at barrier surfaces and beyond. *Immunity* **43**, 15–28.
30 Ivashkiv LB and Donlin LT (2014) Regulation of type I interferon responses. *Nat Rev Immunol* **14**, 36–49.
31 Takeuchi O and Akira S (2009) Innate immunity to virus infection. *Immunol Rev* **227**, 75–86.
32 Kawai T and Akira S (2009) The roles of TLRs, RLRs and NLRs in pathogen recognition. *Int Immunol* **21**, 317–337.
33 Jensen S and Thomsen AR (2012) Sensing of RNA viruses: a review of innate immune receptors involved in recognizing RNA virus invasion. *J Virol* **86**, 2900–2910.
34 Melchjorsen J, Jensen SB, Malmgaard L, Rasmussen SB, Weber F, Bowie AG, Matikainen S and Paludan SR (2005) Activation of innate defense against a paramyxovirus is mediated by RIG-I and TLR7 and TLR8 in a cell-type-specific manner. *J Virol* **79**, 12944–12951.
35 Egli A, Santer DM, O'Shea D, Tyrrell DL and Houghton M (2014) The impact of the interferon-lambda family on the innate and adaptive immune response to viral infections. *Emerg Microbes Infect* **3**, e51.
36 Davis BK, Wen H and Ting JP (2011) The inflammasome NLRs in immunity, inflammation, and associated diseases. *Annu Rev Immunol* **29**, 707–735.
37 Kawai T and Akira S (2010) The role of pattern-recognition receptors in innate immunity: update on Toll-like receptors. *Nat Immunol* **11**, 373–384.
38 Botos I, Segal DM and Davies DR (2011) The structural biology of Toll-like receptors. *Structure* **19**, 447–459.
39 Hornung V, Rothenfusser S, Britsch S, Krug A, Jahrsdörfer B, Giese T, Endres S and Hartmann G (2002) Quantitative expression of toll-like receptor 1-10 mRNA in cellular subsets of human peripheral blood mononuclear cells and sensitivity to CpG oligodeoxynucleotides. *J Immunol* **168**, 4531–4537.
40 Liu L, Botos I, Wang Y, Leonard JN, Shiloach J, Segal DM and Davies DR (2008) Structural basis of toll-like receptor 3 signaling with double-stranded RNA. *Science* **320**, 379–381.
41 Yamamoto M, Sato S, Hemmi H, Hoshino K, Kaisho T, Sanjo H, Takeuchi O, Sugiyama M, Okabe M, Takeda K *et al.* (2003) Role of adaptor TRIF in the MyD88-independent toll-like receptor signaling pathway. *Science* **301**, 640–643.
42 Ono K, Ohtomo T, Sato S, Sugamata Y, Suzuki M, Hisamoto N, Ninomiya-Tsuji J, Tsuchiya M and Matsumoto K (2001) An evolutionarily conserved motif in the TAB 1 C-terminal region is necessary for interaction with and activation of TAK1 MAPKKK. *J Biol Chem* **276**, 24396–24400.
43 Cheung PC, Nebreda AR and Cohen P (2004) TAB 3, a new binding partner of the protein kinase TAK1. *Biochem J* **378**, 27–34.
44 Besse A, Lamothe B, Campos AD, Webster WK, Maddineni U, Lin SC, Wu H and Darnay BG (2007) TAK1-dependent signaling requires functional interaction with TAB 2/TAB 3. *J Biol Chem* **282**, 3918–3928.
45 Wang C, Deng L, Hong M, Akkaraju GR, Inoue J and Chen ZJ (2001) TAK1 is a ubiquitin-dependent kinase of MKK and IKK. *Nature* **412**, 346–351.
46 Tseng PH, Matsuzawa A, Zhang W, Mino T, Vignali DA and Karin M (2010) Different modes of ubiquitination of the adaptor TRAF3 selectively activate the expression of type I interferons and proinflammatory cytokines. *Nat Immunol* **11**, 70–75.
47 Zhao T, Yang L, Sun Q, Arguello M, Ballard DW, Hiscott J and Lin R (2007) The NEMO adaptor bridges the nuclear factor-κB and interferon regulatory factor signaling pathways. *Nat Immunol* **8**, 592–600.
48 Fitzgerald KA, McWhirter SM, Faia KL, Rowe DC, Latz E, Golenbock DT, Coyle AJ, Liao SM and Maniatis T (2003) IKKε and TBK1 are essential components of the IRF3 signaling pathway. *Nat Immunol* **4**, 491–496.
49 tenOever BR, Sharma S, Zou W, Sun Q, Grandvaux N, Julkunen I, Hemmi H, Yamamoto M, Akira S, Yeh WC *et al.* (2004) Activation of TBK1 and IKKε kinases by vesicular stomatitis virus infection and the role of viral ribonucleoprotein in the development of interferon antiviral immunity. *J Virol* **78**, 10636–10649.
50 Medzhitov R, Preston-Hurlburt P, Kopp E, Stadlen A, Chen C, Ghosh S and Janeway CA Jr (1998) MyD88

is an adaptor protein in the hToll/IL-1 receptor family signaling pathways. *Mol Cell* **2**, 253–258.
51 Kawai T and Akira S (2008) Toll-like receptor and RIG-I-like receptor signaling. *Ann N Y Acad Sci* **1143**, 1–20.
52 Yoneyama M, Kikuchi M, Natsukawa T, Shinobu N, Imaizumi T, Miyagishi M, Taira K, Akira S and Fujita T (2004) The RNA helicase RIG-I has an essential function in double-stranded RNA-induced innate antiviral responses. *Nat Immunol* **5**, 730–737.
53 Kang DC, Gopalkrishnan RV, Wu Q, Jankowsky E, Pyle AM and Fisher PB (2002) *mda*-5: an interferon-inducible putative RNA helicase with double-stranded RNA-dependent ATPase activity and melanoma growth-suppressive properties. *Proc Natl Acad Sci USA* **99**, 637–642.
54 Rothenfusser S, Goutagny N, DiPerna G, Gong M, Monks BG, Schoenemeyer A, Yamamoto M, Akira S and Fitzgerald KA (2005) The RNA helicase Lgp2 inhibits TLR-independent sensing of viral replication by retinoic acid-inducible gene-I. *J Immunol* **175**, 5260–5268.
55 Childs K, Randall R and Goodbourn S (2012) Paramyxovirus V proteins interact with the RNA Helicase LGP2 to inhibit RIG-I-dependent interferon induction. *J Virol* **86**, 3411–3421.
56 Deddouche S, Goubau D, Rehwinkel J, Chakravarty P, Begum S, Maillard PV, Borg A, Matthews N, Feng Q, van Kuppeveld FJ *et al*. (2014) Identification of an LGP2-associated MDA5 agonist in picornavirus-infected cells. *Elife* **3**, e01535.
57 Bruns AM, Leser GP, Lamb RA and Horvath CM (2014) The innate immune sensor LGP2 activates antiviral signaling by regulating MDA5-RNA interaction and filament assembly. *Mol Cell* **55**, 771–781.
58 Kato H, Takeuchi O, Sato S, Yoneyama M, Yamamoto M, Matsui K, Uematsu S, Jung A, Kawai T, Ishii KJ *et al*. (2006) Differential roles of MDA5 and RIG-I helicases in the recognition of RNA viruses. *Nature* **441**, 101–105.
59 Cao X, Ding Q, Lu J, Tao W, Huang B, Zhao Y, Niu J, Liu YJ and Zhong J (2015) MDA5 plays a critical role in interferon response during hepatitis C virus infection. *J Hepatol* **62**, 771–778.
60 Kawai T, Takahashi K, Sato S, Coban C, Kumar H, Kato H, Ishii KJ, Takeuchi O and Akira S (2005) IPS-1, an adaptor triggering RIG-I- and Mda5-mediated type I interferon induction. *Nat Immunol* **6**, 981–988.
61 Cai X, Chen J, Xu H, Liu S, Jiang QX, Halfmann R and Chen ZJ (2014) Prion-like polymerization underlies signal transduction in antiviral immune defense and inflammasome activation. *Cell* **156**, 1207–1222.
62 Gack MU, Shin YC, Joo CH, Urano T, Liang C, Sun L, Takeuchi O, Akira S, Chen Z, Inoue S *et al*. (2007) TRIM25 RING-finger E3 ubiquitin ligase is essential for RIG-I-mediated antiviral activity. *Nature* **446**, 916–920.
63 Saha SK, Pietras EM, He JQ, Kang JR, Liu SY, Oganesyan G, Shahangian A, Zarnegar B, Shiba TL, Wang Y *et al*. (2006) Regulation of antiviral responses by a direct and specific interaction between TRAF3 and Cardif. *EMBO J* **25**, 3257–3263.
64 Yoshida R, Takaesu G, Yoshida H, Okamoto F, Yoshioka T, Choi Y, Akira S, Kawai T, Yoshimura A and Kobayashi T (2008) TRAF6 and MEKK1 play a pivotal role in the RIG-I-like helicase antiviral pathway. *J Biol Chem* **283**, 36211–36220.
65 Ting JP, Lovering RC, Alnemri ES, Bertin J, Boss JM, Davis BK, Flavell RA, Girardin SE, Godzik A, Harton JA *et al*. (2008) The NLR gene family: a standard nomenclature. *Immunity* **28**, 285–287.
66 Allen IC, Scull MA, Moore CB, Holl EK, McElvania-TeKippe E, Taxman DJ, Guthrie EH, Pickles RJ and Ting JP (2009) The NLRP3 inflammasome mediates in vivo innate immunity to influenza A virus through recognition of viral RNA. *Immunity* **30**, 556–565.
67 Rajan JV, Rodriguez D, Miao EA and Aderem A (2011) The NLRP3 inflammasome detects encephalomyocarditis virus and vesicular stomatitis virus infection. *J Virol* **85**, 4167–4172.
68 Burdette D, Haskett A, Presser L, McRae S, Iqbal J and Waris G (2012) Hepatitis C virus activates interleukin-1β via caspase-1-inflammasome complex. *J Gen Virol* **93**, 235–246.
69 Strober W and Watanabe T (2011) NOD2, an intracellular innate immune sensor involved in host defense and Crohn's disease. *Mucosal Immunol* **4**, 484–495.
70 Sabbah A, Chang TH, Harnack R, Frohlich V, Tominaga K, Dube PH, Xiang Y and Bose S (2009) Activation of innate immune antiviral responses by Nod2. *Nat Immunol* **10**, 1073–1080.
71 Abbott DW, Yang Y, Hutti JE, Madhavarapu S, Kelliher MA and Cantley LC (2007) Coordinated regulation of Toll-like receptor and NOD2 signaling by K63-linked polyubiquitin chains. *Mol Cell Biol* **27**, 6012–6025.
72 Schultheiss T, Kusov YY and Gauss-Müller V (1994) Proteinase 3C of hepatitis A virus (HAV) cleaves the HAV polyprotein P2-P3 at all sites including VP1/2A and 2A/2B. *Virology* **198**, 275–281.
73 Probst C, Jecht M and Gauss-Müller V (1999) Intrinsic signals for the assembly of hepatitis A virus particles. Role of structural proteins VP4 and 2A. *J Biol Chem* **274**, 4527–4531.
74 Gitlin L, Barchet W, Gilfillan S, Cella M, Beutler B, Flavell RA, Diamond MS and Colonna M (2006) Essential role of mda-5 in type I IFN responses to

polyriboinosinic:polyribocytidylic acid and encephalomyocarditis picornavirus. *Proc Natl Acad Sci USA* **103**, 8459–8464.
75 Oshiumi H, Okamoto M, Fujii K, Kawanishi T, Matsumoto M, Koike S and Seya T (2011) The TLR3/TICAM-1 pathway is mandatory for innate immune responses to poliovirus infection. *J Immunol* **187**, 5320–5327.
76 Wang B, Xi X, Lei X, Zhang X, Cui S, Wang J, Jin Q and Zhao Z (2013) Enterovirus 71 protease $2A^{pro}$ targets MAVS to inhibit anti-viral type I interferon responses. *PLoS Pathog* **9**, e1003231.
77 Feng Q, Langereis MA, Lork M, Nguyen M, Hato SV, Lanke K, Emdad L, Bhoopathi P, Fisher PB, Lloyd RE *et al*. (2014) Enterovirus $2A^{pro}$ targets MDA5 and MAVS in infected cells. *J Virol* **88**, 3369–3378.
78 Lind K, Svedin E, Domsgen E, Kapell S, Laitinen O, Moll M and Flodström-Tullberg M (2016) Coxsackievirus counters the host innate immune response by blocking type III interferon expression. *J Gen Virol* **97**, 1–12.
79 Falah N, Montserret R, Lelogeais V, Schuffenecker I, Lina B, Cortay JC and Violot S (2012) Blocking human enterovirus 71 replication by targeting viral 2A protease. *J Antimicrob Chemother* **67**, 2865–2869.
80 Barral PM, Morrison JM, Drahos J, Gupta P, Sarkar D, Fisher PB and Racaniello VR (2007) MDA-5 is cleaved in poliovirus-infected cells. *J Virol* **81**, 3677–3684.
81 Mukherjee A, Morosky SA, Delorme-Axford E, Dybdahl-Sissoko N, Oberste MS, Wang T and Coyne CB (2011) The coxsackievirus B 3C protease cleaves MAVS and TRIF to attenuate host type I interferon and apoptotic signaling. *PLoS Pathog* **7**, e1001311.
82 Lu J, Yi L, Zhao J, Yu J, Chen Y, Lin MC, Kung HF and He ML (2012) Enterovirus 71 disrupts interferon signaling by reducing the level of interferon receptor 1. *J Virol* **86**, 3767–3776.
83 Liu Y, Zhang Z, Zhao X, Yu R, Zhang X, Wu S, Liu J, Chi X, Song X, Fu L *et al*. (2014) Enterovirus 71 inhibits cellular type I interferon signaling by downregulating JAK1 protein expression. *Viral Immunol* **27**, 267–276.
84 Wang C, Sun M, Yuan X, Ji L, Jin Y, Cardona CJ and Xing Z (2017) Enterovirus 71 suppresses interferon responses by blocking Janus kinase (JAK)/signal transducer and activator of transcription (STAT) signaling through inducing karyopherin-α1 degradation. *J Biol Chem* **292**, 10262–10274.
85 Kerekatte V, Keiper BD, Badorff C, Cai A, Knowlton KU and Rhoads RE (1999) Cleavage of Poly(A)-binding protein by coxsackievirus 2A protease in vitro and in vivo: another mechanism for host protein synthesis shutoff? *J Virol* **73**, 709–717.
86 Novoa I and Carrasco L (1999) Cleavage of eukaryotic translation initiation factor 4G by exogenously added hybrid proteins containing poliovirus $2A^{pro}$ in HeLa cells: effects on gene expression. *Mol Cell Biol* **19**, 2445–2454.
87 Glaser W and Skern T (2000) Extremely efficient cleavage of eIF4G by picornaviral proteinases L and 2A *in vitro*. *FEBS Lett* **480**, 151–155.
88 Blom N, Hansen J, Blaas D and Brunak S (1996) Cleavage site analysis in picornaviral polyproteins: discovering cellular targets by neural networks. *Protein Sci* **5**, 2203–2216.
89 Kusov YY and Gauss-Müller V (1997) In vitro RNA binding of the hepatitis A virus proteinase 3C (HAV $3C^{pro}$) to secondary structure elements within the 5′ terminus of the HAV genome. *RNA* **3**, 291–302.
90 Binford SL, Maldonado F, Brothers MA, Weady PT, Zalman LS, Meador JW, Matthews DA and Patick AK (2005) Conservation of amino acids in human rhinovirus 3C protease correlates with broad-spectrum antiviral activity of rupintrivir, a novel human rhinovirus 3C protease inhibitor. *Antimicrob Agents Chemother* **49**, 619–626.
91 Kuo CJ, Shie JJ, Fang JM, Yen GR, Hsu JT, Liu HG, Tseng SN, Chang SC, Lee CY, Shih SR *et al*. (2008) Design, synthesis, and evaluation of 3C protease inhibitors as anti-enterovirus 71 agents. *Bioorg Med Chem* **16**, 7388–7398.
92 Lei X, Liu X, Ma Y, Sun Z, Yang Y, Jin Q, He B and Wang J (2010) The 3C protein of enterovirus 71 inhibits retinoid acid-inducible gene I-mediated interferon regulatory factor 3 activation and type I interferon responses. *J Virol* **84**, 8051–8061.
93 Papon L, Oteiza A, Imaizumi T, Kato H, Brocchi E, Lawson TG, Akira S and Mechti N (2009) The viral RNA recognition sensor RIG-I is degraded during encephalomyocarditis virus (EMCV) infection. *Virology* **393**, 311–318.
94 Rui Y, Su J, Wang H, Chang J, Wang S, Zheng W, Cai Y, Wei W, Gordy JT, Markham R *et al*. (2017) Disruption of MDA5-mediated innate immune responses by the 3C proteins of coxsackievirus A16, coxsackievirus A6, and enterovirus D68. *J Virol* **91**, e00546–17.
95 Yang Y, Liang Y, Qu L, Chen Z, Yi M, Li K and Lemon SM (2007) Disruption of innate immunity due to mitochondrial targeting of a picornaviral protease precursor. *Proc Natl Acad Sci USA* **104**, 7253–7258.
96 Qian S, Fan W, Liu T, Wu M, Zhang H, Cui X, Zhou Y, Hu J, Wei S, Chen H *et al*. (2017) Seneca Valley Virus suppresses host type I interferon production by targeting adaptor proteins MAVS, TRIF, and TANK for cleavage. *J Virol* **91**, e00823–17.
97 Lei X, Sun Z, Liu X, Jin Q, He B and Wang J (2011) Cleavage of the adaptor protein TRIF by enterovirus

71 3C inhibits antiviral responses mediated by Toll-like receptor 3. *J Virol* **85**, 8811–8818.
98 Xiang Z, Li L, Lei X, Zhou H, Zhou Z, He B and Wang J (2014) Enterovirus 68 3C protease cleaves TRIF to attenuate antiviral responses mediated by Toll-like receptor 3. *J Virol* **88**, 6650–6659.
99 Qu L, Feng Z, Yamane D, Liang Y, Lanford RE, Li K and Lemon SM (2011) Disruption of TLR3 signaling due to cleavage of TRIF by the hepatitis A virus protease-polymerase processing intermediate, 3CD. *PLoS Pathog* **7**, e1002169.
100 Wang D, Fang L, Li K, Zhong H, Fan J, Ouyang C, Zhang H, Duan E, Luo R, Zhang Z *et al.* (2012) Foot-and-mouth disease virus 3C protease cleaves NEMO to impair innate immune signaling. *J Virol* **86**, 9311–9322.
101 Wang D, Fang L, Wei D, Zhang H, Luo R, Chen H, Li K and Xiao S (2014) Hepatitis A virus 3C protease cleaves NEMO to impair induction of beta interferon. *J Virol* **88**, 10252–10258.
102 Guo B and Cheng G (2007) Modulation of the interferon antiviral response by the TBK1/IKKi adaptor protein TANK. *J Biol Chem* **282**, 11817–11826.
103 Chariot A, Leonardi A, Muller J, Bonif M, Brown K and Siebenlist U (2002) Association of the adaptor TANK with the IκB kinase (IKK) regulator NEMO connects IKK complexes with IKKε and TBK1 kinases. *J Biol Chem* **277**, 37029–37036.
104 Deng L, Wang C, Spencer E, Yang L, Braun A, You J, Slaughter C, Pickart C and Chen ZJ (2000) Activation of the IκB kinase complex by TRAF6 requires a dimeric ubiquitin-conjugating enzyme complex and a unique polyubiquitin chain. *Cell* **103**, 351–361.
105 Wang W, Huang X, Xin HB, Fu M, Xue A and Wu ZH (2015) TRAF Family Member-associated NF-κB activator (TANK) inhibits genotoxic nuclear factor κB activation by facilitating deubiquitinase USP10-dependent deubiquitination of TRAF6 ligase. *J Biol Chem* **290**, 13372–13385.
106 Huang L, Liu Q, Zhang L, Zhang Q, Hu L, Li C, Wang S, Li J, Zhang Y, Yu H *et al.* (2015) Encephalomyocarditis virus 3C protease relieves TRAF family member-associated NF-κB activator (TANK) inhibitory effect on TRAF6-mediated NF-κB signaling through cleavage of TANK. *J Biol Chem* **290**, 27618–27632.
107 Huang L, Xiong T, Yu H, Zhang Q, Zhang K, Li C, Hu L, Zhang Y, Zhang L, Liu Q *et al.* (2017) Encephalomyocarditis virus 3C protease attenuates type I interferon production through disrupting the TANK-TBK1-IKKε-IRF3 complex. *Biochem J* **474**, 2051–2065.
108 Lei X, Han N, Xiao X, Jin Q, He B and Wang J (2014) Enterovirus 71 3C inhibits cytokine expression through cleavage of the TAK1/TAB 1/TAB 2/TAB 3 complex. *J Virol* **88**, 9830–9841.
109 Levy DE, Marié I, Smith E and Prakash A (2002) Enhancement and diversification of IFN induction by IRF-7-mediated positive feedback. *J Interferon Cytokine Res* **22**, 87–93.
110 Lei X, Xiao X, Xue Q, Jin Q, He B and Wang J (2013) Cleavage of interferon regulatory factor 7 by enterovirus 71 3C suppresses cellular responses. *J Virol* **87**, 1690–1698.
111 Xiang Z, Liu L, Lei X, Zhou Z, He B and Wang J (2015) 3C protease of enterovirus D68 inhibits cellular defense mediated by interferon regulatory factor 7. *J Virol* **90**, 1613–1621.
112 Fink K and Grandvaux N (2013) STAT2 and IRF9: beyond ISGF3. *JAKSTAT* **2**, e27521.
113 Hung HC, Wang HC, Shih SR, Teng IF, Tseng CP and Hsu JT (2011) Synergistic inhibition of enterovirus 71 replication by interferon and rupintrivir. *J Infect Dis* **203**, 1784–1790.
114 Kuyumcu-Martinez NM, Van Eden ME, Younan P and Lloyd RE (2004) Cleavage of poly(A)-binding protein by poliovirus 3C protease inhibits host cell translation: a novel mechanism for host translation shutoff. *Mol Cell Biol* **24**, 1779–1790.
115 Zhang B, Morace G, Gauss-Müller V and Kusov Y (2007) Poly(A) binding protein, C-terminally truncated by the hepatitis A virus proteinase 3C, inhibits viral translation. *Nucleic Acids Res* **35**, 5975–5984.
116 Clarke BE, Sangar DV, Burroughs JN, Newton SE, Carroll AR and Rowlands DJ (1985) Two initiation sites for foot-and-mouth disease virus polyprotein *in vivo*. *J Gen Virol* **66**, 2615–2626.
117 de Los Santos T, Diaz-San Segundo F and Grubman MJ (2007) Degradation of nuclear factor kappa B during foot-and-mouth disease virus infection. *J Virol* **81**, 12803–12815.
118 de los Santos T, Segundo FD, Zhu J, Koster M, Dias CC and Grubman MJ (2009) A conserved domain in the leader proteinase of foot-and-mouth disease virus is required for proper subcellular localization and function. *J Virol* **83**, 1800–1810.
119 Wang D, Fang L, Luo R, Ye R, Fang Y, Xie L, Chen H and Xiao S (2010) Foot-and-mouth disease virus leader proteinase inhibits dsRNA-induced type I interferon transcription by decreasing interferon regulatory factor 3/7 in protein levels. *Biochem Biophys Res Commun* **399**, 72–78.
120 Medina GN, Knudsen GM, Greninger AL, Kloc A, Díaz-San Segundo F, Rieder E, Grubman MJ, DeRisi JL and de Los Santos T (2017) Interaction between FMDV L^{pro} and transcription factor ADNP is required for optimal viral replication. *Virology* **505**, 12–22.

121 Wang D, Fang L, Li P, Sun L, Fan J, Zhang Q, Luo R, Liu X, Li K, Chen H *et al*. (2011) The leader proteinase of foot-and-mouth disease virus negatively regulates the type I interferon pathway by acting as a viral deubiquitinase. *J Virol* **85**, 3758–3766.
122 Mao AP, Li S, Zhong B, Li Y, Yan J, Li Q, Teng C and Shu HB (2010) Virus-triggered ubiquitination of TRAF3/6 by cIAP1/2 is essential for induction of interferon-β (IFN-β) and cellular antiviral response. *J Biol Chem* **285**, 9470–9476.
123 Neuman BW (2016) Bioinformatics and functional analyses of coronavirus nonstructural proteins involved in the formation of replicative organelles. *Antiviral Res* **135**, 97–107.
124 Lei J, Kusov Y and Hilgenfeld R (2017) Nsp3 of coronaviruses: structures and functions of a large multi-domain protein. *Antiviral Res*, in press.
125 Mielech AM, Kilianski A, Baez-Santos YM, Mesecar AD and Baker SC (2014) MERS-CoV papain-like protease has deISGylating and deubiquitinating activities. *Virology* **450–451**, 64–70.
126 Báez-Santos YM, Barraza SJ, Wilson MW, Agius MP, Mielech AM, Davis NM, Baker SC, Larsen SD and Mesecar AD (2014) X-ray structural and biological evaluation of a series of potent and highly selective inhibitors of human coronavirus papain-like proteases. *J Med Chem* **57**, 2393–2412.
127 Li Y, Chen M, Cao H, Zhu Y, Zheng J and Zhou H (2013) Extraordinary GU-rich single-strand RNA identified from SARS coronavirus contributes an excessive innate immune response. *Microbes Infect* **15**, 88–95.
128 Li SW, Wang CY, Jou YJ, Huang SH, Hsiao LH, Wan L, Lin YJ, Kung SH and Lin CW (2016) SARS coronavirus papain-Like protease inhibits the TLR7 signaling pathway through removing Lys63-linked polyubiquitination of TRAF3 and TRAF6. *Int J Mol Sci* **17**, E678.
129 Békés M, van der Heden van Noort GJ, Ekkebus R, Ovaa H, Huang TT and Lima CD (2016) Recognition of Lys48-linked di-ubiquitin and deubiquitinating activities of the SARS coronavirus papain-like protease. *Mol Cell* **62**, 572–585.
130 Sun W, Li Y, Chen L, Chen H, You F, Zhou X, Zhou Y, Zhai Z, Chen D and Jiang Z (2009) ERIS, an endoplasmic reticulum IFN stimulator, activates innate immune signaling through dimerization. *Proc Natl Acad Sci USA* **106**, 8653–8658.
131 Ishikawa H and Barber GN (2008) STING is an endoplasmic reticulum adaptor that facilitates innate immune signalling. *Nature* **455**, 674–678.
132 Sun L, Xing Y, Chen X, Zheng Y, Yang Y, Nichols DB, Clementz MA, Banach BS, Li K, Baker SC *et al*. (2012) Coronavirus papain-like proteases negatively regulate antiviral innate immune response through disruption of STING-mediated signaling. *PLoS One* **7**, e30802.
133 Chen X, Yang X, Zheng Y, Yang Y, Xing Y and Chen Z (2014) SARS coronavirus papain-like protease inhibits the type I interferon signaling pathway through interaction with the STING-TRAF3-TBK1 complex. *Protein Cell* **5**, 369–381.
134 Devaraj SG, Wang N, Chen Z, Chen Z, Tseng M, Barretto N, Lin R, Peters CJ, Tseng CT, Baker SC *et al*. (2007) Regulation of IRF-3-dependent innate immunity by the papain-like protease domain of the severe acute respiratory syndrome coronavirus. *J Biol Chem* **282**, 32208–32221.
135 Wang G, Chen G, Zheng D, Cheng G and Tang H (2011) PLP2 of mouse hepatitis virus A59 (MHV-A59) targets TBK1 to negatively regulate cellular type I interferon signaling pathway. *PLoS One* **6**, e17192.
136 Zheng D, Chen G, Guo B, Cheng G and Tang H (2008) PLP2, a potent deubiquitinase from murine hepatitis virus, strongly inhibits cellular type I interferon production. *Cell Res* **18**, 1105–1113.
137 Muñoz-Fontela C, Macip S, Martínez-Sobrido L, Brown L, Ashour J, García-Sastre A, Lee SW and Aaronson SA (2008) Transcriptional role of p53 in interferon-mediated antiviral immunity. *J Exp Med* **205**, 1929–1938.
138 Yuan L, Chen Z, Song S, Wang S, Tian C, Xing G, Chen X, Xiao ZX, He F and Zhang L (2015) p53 degradation by a coronavirus papain-like protease suppresses type I interferon signaling. *J Biol Chem* **290**, 3172–3182.
139 Ma-Lauer Y, Carbajo-Lozoya J, Hein MY, Müller MA, Deng W, Lei J, Meyer B, Kusov Y, von Brunn B, Bairad DR *et al*. (2016) p53 down-regulates SARS coronavirus replication and is targeted by the SARS-unique domain and PL^{pro} via E3 ubiquitin ligase RCHY1. *Proc Natl Acad Sci USA* **113**, E5192–E5201.
140 Frieman M, Ratia K, Johnston RE, Mesecar AD and Baric RS (2009) Severe acute respiratory syndrome coronavirus papain-like protease ubiquitin-like domain and catalytic domain regulate antagonism of IRF3 and NF-κB signaling. *J Virol* **83**, 6689–6705.
141 Clementz MA, Chen Z, Banach BS, Wang Y, Sun L, Ratia K, Baez-Santos YM, Wang J, Takayama J, Ghosh AK *et al*. (2010) Deubiquitinating and interferon antagonism activities of coronavirus papain-like proteases. *J Virol* **84**, 4619–4629.
142 Shi CS, Shenderov K, Huang NN, Kabat J, Abu-Asab M, Fitzgerald KA, Sher A and Kehrl JH (2012) Activation of autophagy by inflammatory signals limits IL-1β production by targeting ubiquitinated inflammasomes for destruction. *Nat Immunol* **13**, 255–263.
143 Chen X, Wang K, Xing Y, Tu J, Yang X, Zhao Q, Li K and Chen Z (2014) Coronavirus membrane-

associated papain-like proteases induce autophagy through interacting with Beclin1 to negatively regulate antiviral innate immunity. *Protein Cell* **5**, 912–927.
144 Zhu L, George S, Schmidt MF, Al-Gharabli SI, Rademann J and Hilgenfeld R (2011) Peptide aldehyde inhibitors challenge the substrate specificity of the SARS-coronavirus main protease. *Antiviral Res* **92**, 204–212.
145 Pillaiyar T, Manickam M, Namasivayam V, Hayashi Y and Jung SH (2016) An overview of severe acute respiratory syndrome-coronavirus (SARS-CoV) 3CL protease inhibitors: peptidomimetics and small molecule chemotherapy. *J Med Chem* **59**, 6595–6628.
146 Wang D, Fang L, Shi Y, Zhang H, Gao L, Peng G, Chen H, Li K and Xiao S (2015) Porcine epidemic diarrhea virus 3C-like protease regulates its interferon antagonism by cleaving NEMO. *J Virol* **90**, 2090–2101.
147 Zhu X, Fang L, Wang D, Yang Y, Chen J, Ye X, Foda MF and Xiao S (2017) Porcine deltacoronavirus nsp5 inhibits interferon-β production through the cleavage of NEMO. *Virology* **502**, 33–38.
148 Zhu X, Wang D, Zhou J, Pan T, Chen J, Yang Y, Lv M, Ye X, Peng G, Fang L *et al*. (2017) Porcine deltacoronavirus nsp5 antagonizes type I interferon signaling by cleaving STAT2. *J Virol* **91**, e00003–17.
149 Lawitz E, Sulkowski MS, Ghalib R, Rodriguez-Torres M, Younossi ZM, Corregidor A, DeJesus E, Pearlman B, Rabinovitz M, Gitlin N *et al*. (2014) Simeprevir plus sofosbuvir, with or without ribavirin, to treat chronic infection with hepatitis C virus genotype 1 in non-responders to pegylated interferon and ribavirin and treatment-naïve patients: the COSMOS randomised study. *Lancet* **384**, 1756–1765.
150 Zeuzem S, Jacobson IM, Baykal T, Marinho RT, Poordad F, Bourlière M, Sulkowski MS, Wedemeyer H, Tam E, Desmond P *et al*. (2014) Retreatment of HCV with ABT-450/r-ombitasvir and dasabuvir with ribavirin. *N Engl J Med* **370**, 1604–1614.
151 Sumpter R Jr, Loo YM, Foy E, Li K, Yoneyama M, Fujita T, Lemon SM and Gale M Jr (2005) Regulating intracellular antiviral defense and permissiveness to hepatitis C virus RNA replication through a cellular RNA helicase, RIG-I. *J Virol* **79**, 2689–2699.
152 Meylan E, Curran J, Hofmann K, Moradpour D, Binder M, Bartenschlager R and Tschopp J (2005) Cardif is an adaptor protein in the RIG-I antiviral pathway and is targeted by hepatitis C virus. *Nature* **437**, 1167–1172.
153 Chen Z, Benureau Y, Rijnbrand R, Yi J, Wang T, Warter L, Lanford RE, Weinman SA, Lemon SM, Martin A *et al*. (2007) GB virus B disrupts RIG-I signaling by NS3/4A-mediated cleavage of the adaptor protein MAVS. *J Virol* **81**, 964–976.
154 Anggakusuma, Brown RJ, Banda DH, Todt D, Vieyres G, Steinmann E and Pietschmann T (2016) Hepacivirus NS3/4A proteases interfere with MAVS signaling in both their cognate animal hosts and humans: implications for zoonotic transmission. *J Virol* **90**, 10670–10681.
155 Oshiumi H, Miyashita M, Matsumoto M and Seya T (2013) A distinct role of Riplet-mediated K63-Linked polyubiquitination of the RIG-I repressor domain in human antiviral innate immune responses. *PLoS Pathog* **9**, e1003533.
156 Li K, Li NL, Wei D, Pfeffer SR, Fan M and Pfeffer LM (2012) Activation of chemokine and inflammatory cytokine response in hepatitis C virus-infected hepatocytes depends on Toll-like receptor 3 sensing of hepatitis C virus double-stranded RNA intermediates. *Hepatology* **55**, 666–675.
157 Li K, Foy E, Ferreon JC, Nakamura M, Ferreon AC, Ikeda M, Ray SC, Gale M Jr and Lemon SM (2005) Immune evasion by hepatitis C virus NS3/4A protease-mediated cleavage of the Toll-like receptor 3 adaptor protein TRIF. *Proc Natl Acad Sci USA* **102**, 2992–2997.
158 Dansako H, Ikeda M and Kato N (2007) Limited suppression of the interferon-β production by hepatitis C virus serine protease in cultured human hepatocytes. *FEBS J* **274**, 4161–4176.
159 Gagné B, Tremblay N, Park AY, Baril M and Lamarre D (2017) Importin β1 targeting by hepatitis C virus NS3/4A protein restricts IRF3 and NF-κB signaling of IFNB1 antiviral response. *Traffic* **18**, 362–377.
160 Yin Z, Patel SJ, Wang WL, Chan WL, Ranga Rao KR, Wang G, Ngew X, Patel V, Beer D, Knox JE *et al*. (2006) Peptide inhibitors of dengue virus NS3 protease. Part 2: SAR study of tetrapeptide aldehyde inhibitors. *Bioorg Med Chem Lett* **16**, 40–43.
161 Nitsche C, Zhang L, Weigel LF, Schilz J, Graf D, Bartenschlager R, Hilgenfeld R and Klein CD (2017) Peptide-boronic acid inhibitors of flaviviral proteases: medicinal chemistry and structural biology. *J Med Chem* **60**, 511–516.
162 Boldescu V, Behnam MAM, Vasilakis N and Klein CD (2017) Broad-spectrum agents for flaviviral infections: dengue, Zika and beyond. *Nat Rev Drug Discov* **16**, 565–586.
163 Aguirre S, Maestre AM, Pagni S, Patel JR, Savage T, Gutman D, Maringer K, Bernal-Rubio D, Shabman RS, Simon V *et al*. (2012) DENV inhibits type I IFN production in infected cells by cleaving human STING. *PLoS Pathog* **8**, e1002934.
164 Yu CY, Chang TH, Liang JJ, Chiang RL, Lee YL, Liao CL and Lin YL (2012) Dengue virus targets the adaptor protein MITA to subvert host innate immunity. *PLoS Pathog* **8**, e1002780.
165 Liu H, Zhang L, Sun J, Chen W, Li S, Wang Q, Yu H, Xia Z, Jin X and Wang C (2017) Endoplasmic reticulum protein SCAP inhibits dengue virus NS2B3

protease by suppressing its K27-linked polyubiquitylation. *J Virol* **91**, e02234–16.
166 Onoguchi K, Onomoto K, Takamatsu S, Jogi M, Takemura A, Morimoto S, Julkunen I, Namiki H, Yoneyama M and Fujita T (2010) Virus-infection or 5′ppp-RNA activates antiviral signal through redistribution of IPS-1 mediated by MFN1. *PLoS Pathog* **6**, e1001012.
167 Yu CY, Liang JJ, Li JK, Lee YL, Chang BL, Su CI, Huang WJ, Lai MM and Lin YL (2015) Dengue virus impairs mitochondrial fusion by cleaving mitofusins. *PLoS Pathog* **11**, e1005350.
168 Gottipati K, Ruggli N, Gerber M, Tratschin JD, Benning M, Bellamy H and Choi KH (2013) The structure of classical swine fever virus N^{pro}: a novel cysteine autoprotease and zinc-binding protein involved in subversion of type I interferon induction. *PLoS Pathog* **9**, e1003704.
169 Bauhofer O, Summerfield A, Sakoda Y, Tratschin JD, Hofmann MA and Ruggli N (2007) Classical swine fever virus N^{pro} interacts with interferon regulatory factor 3 and induces its proteasomal degradation. *J Virol* **81**, 3087–3096.
170 Gottipati K, Holthauzen LM, Ruggli N and Choi KH (2016) Pestivirus N^{pro} directly interacts with interferon regulatory factor 3 monomer and dimer. *J Virol* **90**, 7740–7747.
171 Hilton L, Moganeradj K, Zhang G, Chen YH, Randall RE, McCauley JW and Goodbourn S (2006) The N^{pro} product of bovine viral diarrhea virus inhibits DNA binding by interferon regulatory factor 3 and targets it for proteasomal degradation. *J Virol* **80**, 11723–11732.
172 Chen Z, Rijnbrand R, Jangra RK, Devaraj SG, Qu L, Ma Y, Lemon SM and Li K (2007) Ubiquitination and proteasomal degradation of interferon regulatory factor-3 induced by N^{pro} from a cytopathic bovine viral diarrhea virus. *Virology* **366**, 277–292.
173 Szymanski MR, Fiebach AR, Tratschin JD, Gut M, Ramanujam VM, Gottipati K, Patel P, Ye M, Ruggli N and Choi KH (2009) Zinc binding in pestivirus N^{pro} is required for interferon regulatory factor 3 interaction and degradation. *J Mol Biol* **391**, 438–449.
174 Mine J, Tamura T, Mitsuhashi K, Okamatsu M, Parchariyanon S, Pinyochon W, Ruggli N, Tratschin JD, Kida H, Sakoda Y *et al.* (2015) The N-terminal domain of N^{pro} of classical swine fever virus determines its stability and regulates type I IFN production. *J Gen Virol* **96**, 1746–1756.
175 Fiebach AR, Guzylack-Piriou L, Python S, Summerfield A and Ruggli N (2011) Classical swine fever virus N^{pro} limits type I interferon induction in plasmacytoid dendritic cells by interacting with interferon regulatory factor 7. *J Virol* **85**, 8002–8011.
176 Doceul V, Charleston B, Crooke H, Reid E, Powell PP and Seago J (2008) The N^{pro} product of classical swine fever virus interacts with IκBα, the NF-κB inhibitor. *J Gen Virol* **89**, 1881–1889.
177 Tan CW, Lai JK, Sam IC and Chan YF (2014) Recent developments in antiviral agents against enterovirus 71 infection. *J Biomed Sci* **21**, 14.
178 de Wit E, van Doremalen N, Falzarano D and Munster VJ (2016) SARS and MERS: recent insights into emerging coronaviruses. *Nat Rev Microbiol* **14**, 523–534.
179 Du H, Yin P, Yang X, Zhang L, Jin Q and Zhu G (2015) Enterovirus 71 2C protein inhibits NF-κB activation by binding to RelA(p65). *Sci Rep* **5**, 14302.
180 Dodd DA, Giddings TH Jr and Kirkegaard K (2001) Poliovirus 3A protein limits interleukin-6 (IL-6), IL-8, and beta interferon secretion during viral infection. *J Virol* **75**, 8158–8165.
181 Noguchi T, Satoh S, Noshi T, Hatada E, Fukuda R, Kawai A, Ikeda S, Hijikata M and Shimotohno K (2001) Effects of mutation in hepatitis C virus nonstructural protein 5A on interferon resistance mediated by inhibition of PKR kinase activity in mammalian cells. *Microbiol Immunol* **45**, 829–840.
182 Taylor DR, Shi ST, Romano PR, Barber GN and Lai MM (1999) Inhibition of the interferon-inducible protein kinase PKR by HCV E2 protein. *Science* **285**, 107–110.
183 Pettersen EF, Goddard TD, Huang CC, Couch GS, Greenblatt DM, Meng EC and Ferrin TE (2004) UCSF Chimera — a visualization system for exploratory research and analysis. *J Comput Chem* **25**, 1605–1612.